3D-PRINTED LIGHTWEIGHT WEARABLE MICROSYSTEMS WITH HIGHLY CONDUCTIVE INTERCONNECTS

By

Ahmad Fudy Alforidi

A DISSERTATION

Submitted to
Michigan State University
in partial fulfillment of the requirements
for the degree of

Electrical Engineering -- Doctor of Philosophy

2019

ABSTRACT

3D-PRINTED LIGHTWEIGHT WEARABLE MICROSYSTEMS WITH HIGHLY CONDUCTIVE INTERCONNECTS

By

Ahmad Fudy Alforidi

There is great demand for mass production of electronics in wide range of applications including, but not limited to, ubiquitous and lightweight wearable devices for the development of smart homes and health monitoring systems. The advancement of additive manufacturing in electronics industry and academia shows a potential replacement of conventional electronics fabrication methods. However, conductivity is the most difficult issue towards the implementation of high-performance 3D-printed microsystems. As most of 3D printing electronics utilizes ink-based conductive material for electrical connection, it requires high curing temperature for achieving low resistivity (150 °C for obtaining nearly 2.069 x 10^{-6} Ω.m in copper connects), which is not suitable for most of 3D printing filaments. This seriously limits the availability of many lightweight 3D printable materials in microsystem applications because these materials usually have relatively low glass-transition temperatures (<120 ^{o}C). Considering that pristine copper films thicker than 49 nm can offer a very low bulk resistivity of 1.67 x10^{-8} Ω.m, a new 3D-printing-compatible connection fabrication approach capable of depositing pristine copper structures with no need of curing processes is highly desirable. Therefore, a new technology with the ability to manufacture 3D-printed structures with high performance electronics is necessary.

In this dissertation, novel 3D-printed metallization processes for multilayer microsystems made of lightweight material on planar and non-planar surfaces are presented. The incorporation of metal interconnects in the process is accomplished through evaporating, sputtering and electroplating techniques. This approach involves the following critical processes with unique features: a) patterning of metal interconnects using self-aligned 3D-printed shadow masks, b) fabrication of the temporary connections between isolated metal segments by 3D printing followed with metallization, which host the subsequent electroplating process, and c) fabrication of vertical interconnect access (VIA) features by 3D printing followed with metallization, which enable electrical connections between multilayers of the Microsystem for miniaturization

The presented technique offers approximate bulk resistivity with no curing temperature needed after deposition. Since the ultimate goal is developing lightweight wearable microsystem, this approach demonstrated for two layers and can easily extended for multilayer microsystems enabling realization and miniaturization of complex systems. In addition, the variety of filaments used in 3D-printers provide opportunities to study implementation of these processes in many electronics fields including flexible electronics. Therefore, the integration of physical vapor deposition systems with 3D printing machines is very promising for the future industry of 3D-printed microsystems.

Copyright by
AHMAD FUDY ALFORIDI
2019

This dissertation is dedicated to my beloved family….

ACKNOWLEDGMENTS

I would like to take this opportunity to express my sincere appreciation for all the support and encouragement that have led to the completion of this dissertation. I am greatly indebted to my advisor, Prof. Dean Aslam, for his continuous support, help, patience, and encouragement throughout my PhD studies at Michigan State University. Without his guidance and persistent help and support this dissertation would not have been possible.

I would also like to thank Dr. Wen Li, Dr. Jian Ren, and Dr. Chunqi Qian for serving on my committee. I am deeply grateful to them for their valuable comments and insightful discussion.

Special thanks to our research partners at University of Michigan Prof. Xiaogan Liang and Dr. Da Li for their collaboration and valuable discussions.

I am grateful to Taibah University and the ministry of higher education in Saudi Arabia for providing me a generous fellowship which made it possible for me to pursue my higher education studies at Michigan State University.

I am greatly grateful to my family and friends for their tremendous support and encouragement. My profound gratitude is to my parents Fudy Alfuraydi and khaira Alfuraydi for their endless love, prayers and support.

I could not be more grateful to my beloved wife Shatha and my lovely son Ryan. This dissertation would not have been accomplished without their love, patience, and support. Thank you all for making this dream a reality.

TABLE OF CONTENTS

LIST OF TABLES

LIST OF FIGURES

Chapter 1 Research Motivation and Goals

1.1 Introduction

3D-printing, also known as additive manufacturing, is defined as the process of creating 3D object layer by layer. It was developed in the last three decades for rapid prototyping. Due to the limitations of the 3D-printing technology it was only used for developing conceptual models. It helps visualizing actual complex products to avoid critical design errors or inspire better product design. With the recent advancement of this technology, it became an essential manufacturing process for many applications. In education, 3D printer has become available in many schools to further enhance the creativity of their students. In buildings, 3D printing houses are recently developed with very low cost and completed within few days. Nowadays, 3D-printers are being used in food industry for creating unique structures and shapes of biscuits and chocolates. In fashion industry, 3D-printer is utilized in the fabrication of fashion apparels and jewellery. In electronics industry, 3D-printing electronics has gain significant interest due to the possibility of manufacturing microsystems on planar and non-planar surfaces. In addition, 3D-printing technology facilitae new and innovative products with embedded and streachable electronics. As compared to traditional electronics fabrication methodes, 3D-printing electronics avoid utilizing chemical substances creating eco-friendly manufacturing process.

Development of lightweight wearable devices [1][2] and replacement of conventional fabrication methods for electronic devices [3][4][5][6][7] have led to 3D-printed prosthetics [8], dental implants [9], bionic ears [10], compound eye system [11], antennas [12] and Li-ion microbatteries [13]. However, most of 3D printed microsystems use Cu conductive ink requiring

high curing temperatures to lower the resistivity as shown in figure 1.2 [14] [15]. The copper films offer approximate bulk resistivity of 1.67 x10-8 Ω.m if the thickness of film is 49 nm or larger [16] with no curing temperature needed after deposition. Broader types of materials on plastic substrates with evaporation techniques [17][18] and recent development in 3D printing machines, with ability to print very high-resolution geometrics with different materials, including Acrylonitrile Butadience Styrene (ABS), flexible filaments, High Impact Polystyrene (HIPS) and carbon fiber filaments [20][21][22] are important.

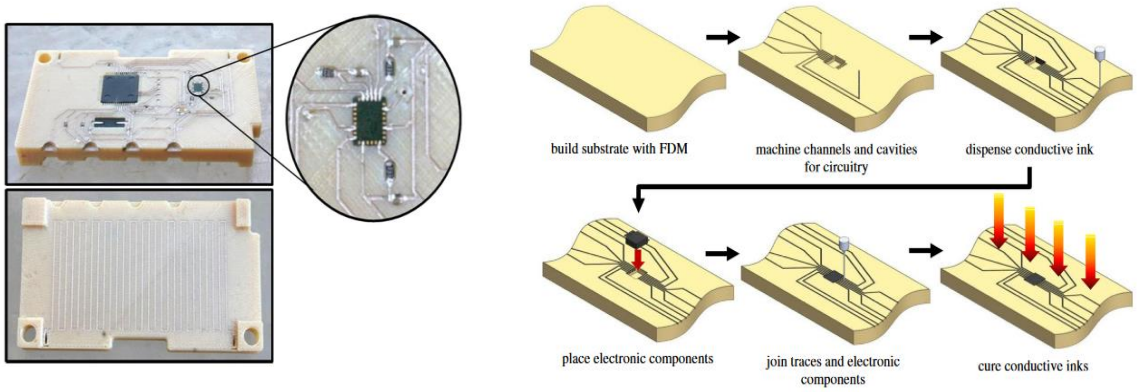

Figure 1. 1: 3D-printed electronics using conductive inks [72].

A)

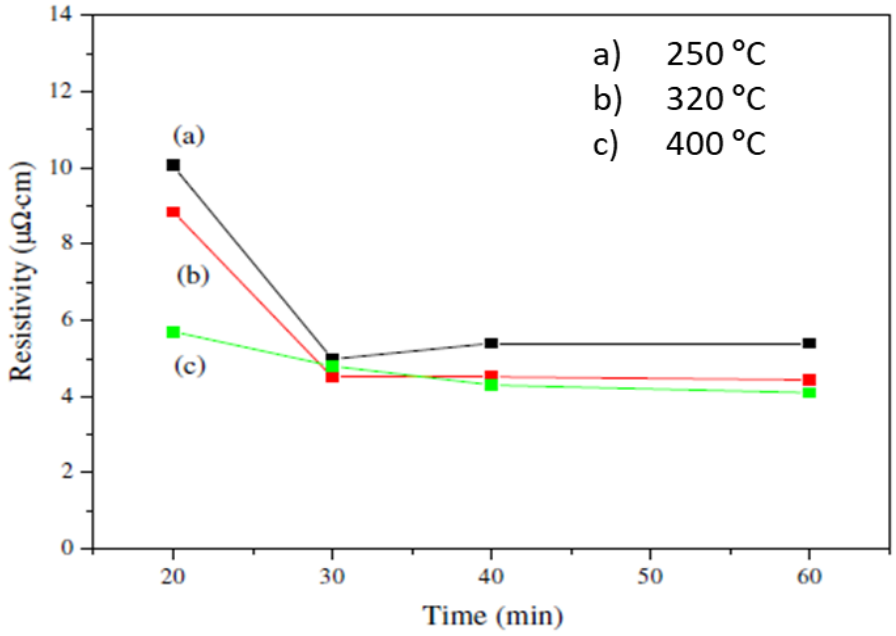

B)

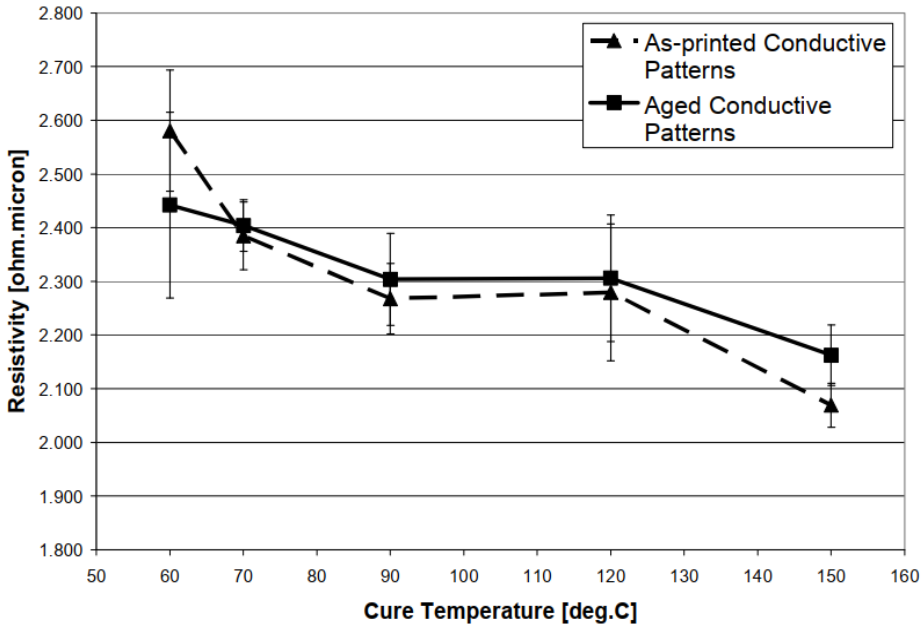

Figure 1. 2: effects of curing at different temperatures on the resistivity of the deposited conductive inks.

1.2 Objective of This Work

Previous work on 3D-printed devices has successfully demonstrated the advantages of mass production non-traditional electronics manufacturing. Being in an early stage of 3D-printing electronics research, these studies are developed through conductive ink-based material, which requires curing at high temperature to achieve approximate bulk resistivity. To be able to overcoming this issue, it is necessary to develop new technology or process capable of implementing high performance 3D- printed microsystem. To apply the new technology, it is important to develop a working microsystem with traditional technology. Therefore, to achieve these objectives, one has to address the following issues:

- The development of fabrication process for patterning conductive metal films on plastic substrate.
- The design and implementation process for multilayer microsystems
- The application of the developed fabrication process in fabric-embedded IEM.

Fig 1.3 illustrates several tasks to be done in order to realize the lightweight wearable microsystem processes.

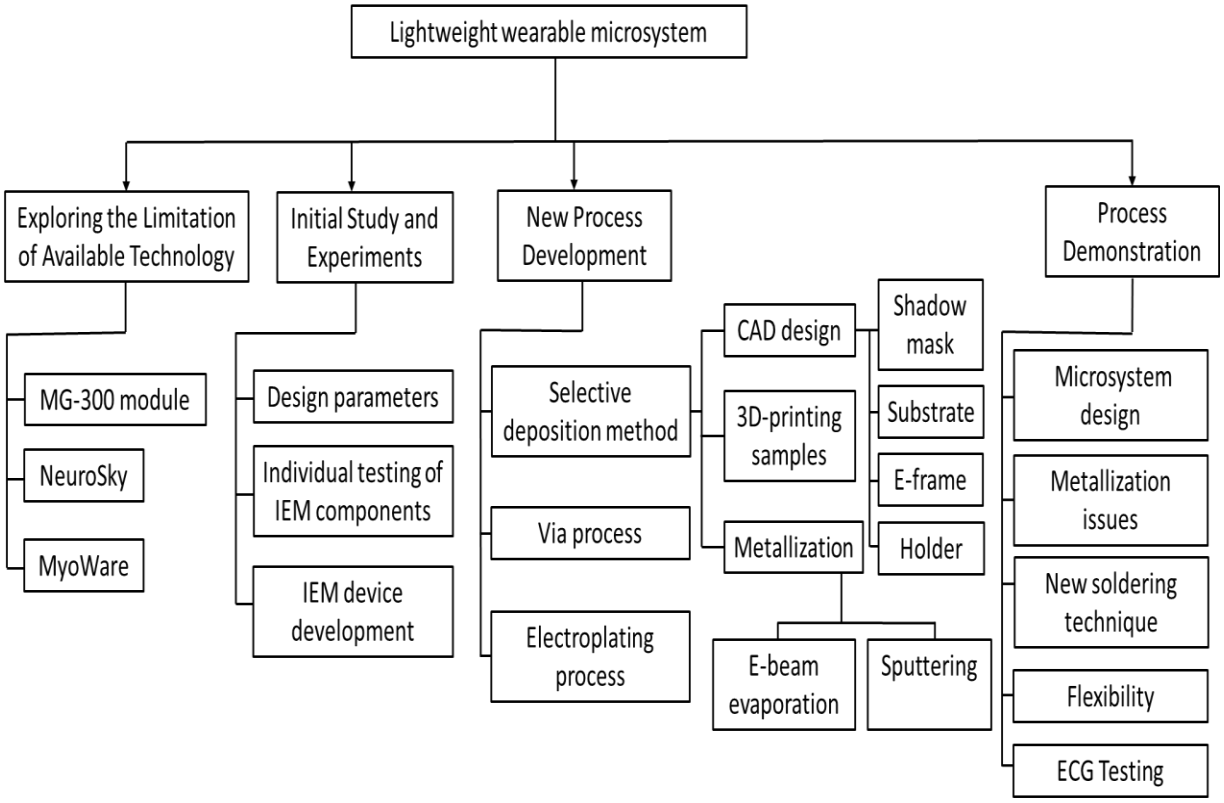

Figure 1. 3: An overview of the development of lightweight wearable microsystems.

1.3 Unique Aspects and Contribution

In this dissertation, novel 3-D printed metallization processes developed for multilayer Microsystems, using lightweight material on planar and non-planar surfaces, for the first time. It has following unique features:

a. Self-aligned 3D-printed shadow mask designed for patterning metal interconnects.

b. A temporary connection between isolated metal segments created by a 3D-printed metalized structure for electroplating process.

c. Vertical interconnect access (via) process created and metalized to enable electrical connection between multilayers of the Microsystem for miniaturization.

d. Initial development of flexible electronics using the presented processes.

e. Components assembly using sputtering and shadow mask with designated aperture allowing evaporated particles to connect leads of surface mount devices with deposited films.

f. This process can be adapted in PCB (Printed Circuit Board) manufacturing as it offers smaller fabrication steps than conventional PCB fabrication.

1.4 Dissertation Organization

In Chapter 1, goals and motivations of this research are described. An overview of the most recent research on wearable devices including bio signals detection, sensors and health monitoring devices are presented in chapter 2. Chapter 3 deals with the exploratory study of available devices to determine limitations and/or possible improvement to address them in this work. It also include the initial design and demonstration of integrated EEG/ECG/EMG microsystem (IEM) for health monitoring. Chapter 4 focusses on the development of 3D-printed microsystem fabrication processes. In chapter 5, application of the new technology is demonstrated on two layers microsystem for Electrocardiogram (ECG) measurements. Summary, conclusion and future work are presented in chapter 6.

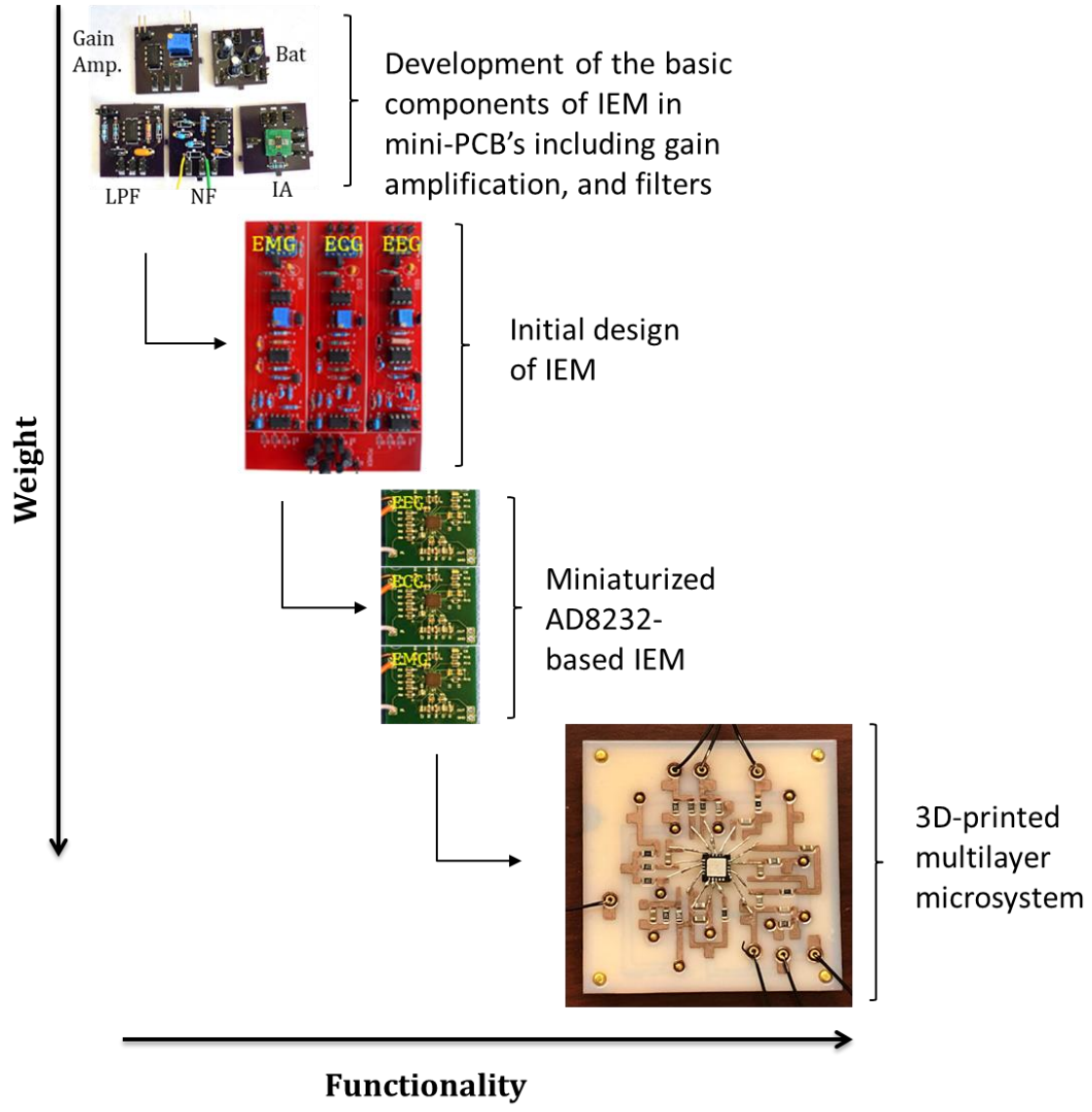

Figure 1. 4: Design flow of the developed lightweight wearable microsystems.

Chapter 2 Background

2.1 Introduction

This chapter presents the fundamental and the current IEM-related research efforts in the last two decades. After reviewing bio signal devices issues (in health monitoring and smart home), various instruments and applications are summarized. General wearable devices that include bio signals detection such as EEG, ECG and EMG are briefly discussed.

The new research on smart home Microsystems is no more limited to Internet-of-Things (IoT) but also includes in-home health and disease monitoring [23][24]. The Brain Computer Interface (BCI) has been widely researched for automating smart home appliances [25][26] [27]. Human Computer Interaction (HCI) has led to multimodal interaction and game research [28]. A study was conducted to determine student attention level during classes using their brain signal from mobile sensors [29]. Based on the brain activity; certain range of frequency becomes more dominant in the measured signal than others. The brain signals categorized based on frequency band into five groups; delta (0.5-4 Hz), theta (4-8 Hz), alpha (8-13 Hz), beta (13-30 Hz) and gamma (above 30). Each of these frequency bands represents the status of the brain. For example, alpha rhythm becomes dominant in the brain signal during relaxation or closing eyes. Beta band appears during alertness and highly focusing on certain things. Sleeping stages represented by the dominants of theta and delta bands in the raw EEG signal. The lower the frequency, the deeper the sleeping. GA-Fisher classifier was implemented on EEG signal to classify four emotions: excitement, fear, oscitancy and awaking [30]. In addition, there is significant development in the field of medical science that led to light weighted and portable biomedical instruments [31][32][33].

2.2 Wearable Devices

Researches in the field of wearable devices for health monitoring have been increasing due to the effectiveness of these devices in tracking vital signs of patients and the increasing cost of healthcare systems. One of the main advantages of wearable devices is the possibility for physicians to get access of the patient's health status when they are out of the hospital. These devices are able to be implemented and operational non-invasively to track the patient's health continuously by connecting with certain signal carrying terminals. Moreover, they are capable to detect a critical physiological data such as electrocardiogram (ECG, heart rate), Electromyography (EMG), Electroencephalography (EEG), blood pressure, shivering, skin color, respiration and temperature. As can be seen in fig. 2.1, the general system level of a bio-signal wearable device consists of four main blocks: sensors, signal conditioning (SC), analog digital converter (ADC), and power management (PM).

There are certain factors need to be considered in the design of wearable devices such as affordability. The wearable device should consider minimizing the cost to the minimum with maintaining high performance so it can be affordable to a large number of consumers in need. In addition, the system's weight and size are major factors of a good wearable device. By reaching a minimum size wearable device, it becomes more comfortable to wear. Furthermore, it's important to keep the patients privacy as priority in wearable devices due to the sensitivity of the collected data. Moreover, in order to sustain longer battery life of the device, it might be necessary to consider different power options such as energy harvesters that include, but not limited to, solar power, thermal energy and kinetic energy.

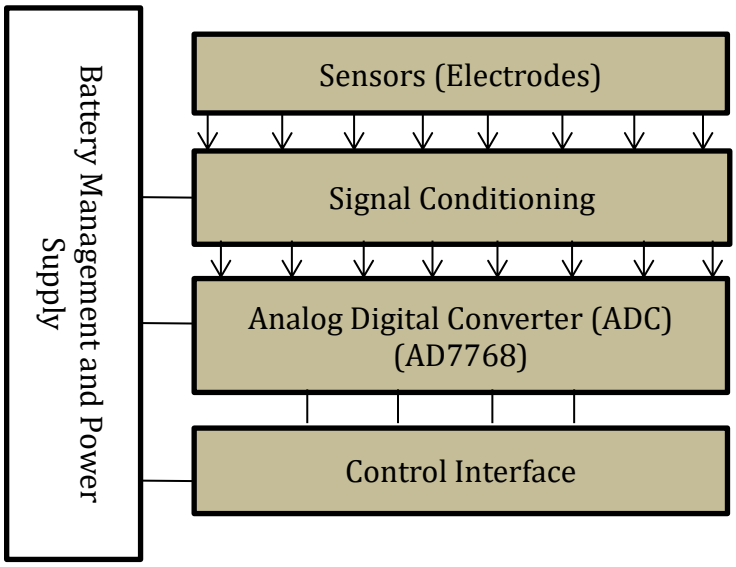

Figure 2. 1: General block diagram of components of wearable devices.

LiveNet [34] is one of the developed wearable systems for health monitoring applications with real time data processing. It incorporates 3D accelerometer, ECG and EMG. It's applied in studies including soldier's health monitoring in brutal environment, monitoring and improving clinical assessment of a Parkinson's patient and epilepsy seizure detection. AMON "A Wearable Multiparameter Medical Monitoring and Alert System." It's a wrist worn device that monitors people with heart and respiratory diseases [35]. It also measures blood pressure and SpO2. RTWPMS [36] is a design and implementation device for monitoring heart rate, blood pressure and temperature. LifeGuard monitoring system capable of detecting vital signs and getting real time wireless data streaming was developed [37]. It detects and measures ECG, respiration, SpO2, and blood pressure. A prototype device capable of measuring ECG/PCG and temperature using PDA and Bluetooth technology was proved feasible in [38]. INA128 was used for all ECG amplification needed. A medical wearable device measures blood oxygen saturation, heart rate,

respiration rate and movement was developed [39]. In [40], an approach of ECG continues measurement was implemented on a wearable belt. A wearable garment capable of acquiring bio signal measurement such as ECG and worn under clothes was implemented [41]. Measurement of electrocardiogram (ECG), Photoplethysmogram (PPG), body temperature, blood pressure, galvanic skin response (GSR) and heart rate were reported in smart vest [42]. In [43], WWBAN prototype was implemented to collect ECG, accelerometer and foot switch data. Design of biosensor boards measuring pulse oximetry, ECG, EMG and motion activity was implemented along with the development of CodeBlue at Harvard University [44]. In [45], ECG was transmitted using Body Area Network (BAN) system. Monitoring critical ECG and blood pressure was implemented in [46]. The abnormal readings can be sent to the emergency. Body sensor network including ECG, photoplethysmogram (PPG) and phonocardiography (PCG) are presented in [47]. BASUMA system is a wearable wireless medical sensor measuring ECG, air and blood content of the thorax, body temperature, breathing rate and cough control, blood pressure, pulse rate, oxygen saturation and lung functions was developed [48]. Human ++ research project [49] focuses on the future wireless BAN's for health monitoring applications including ECG/EEG/EMG. In [68], a programmable analog front-end IC with 7.4 uW power consumption and circuit area of 0.38mm^2 is developed for biomedical applications. It was developed in 2009 but still not available in the market.

Cell phone-based wearable platform continuously recording ECG and automatically detects abnormal cardiovascular (CVD) disease was implemented in [50]. In [51], a mobile phone application capable of detecting critical stage of ECG signal and urge the patient to call emergency immediately. It also capable of determining the patient's location and automatically call the emergency if needed. By targeting subjects under extreme stress and patients with neurological

and psychological disorders, a system was developed to evaluate the emotional state of a human being using classification of EMG and ECG activities [52]. Using ECG signal, motion artifacts was detected to classify the body movement activities [53]. A prototype of gloves with sensors was developed to detect emotions through measuring heart rate, skin conductivity and skin temperature [54]. Wearable ECG and skin temperature monitor were developed using a flexible hybrid electronics technology [57].

The use of remote monitoring for healthcare has great advantages especially for those who lives in rural areas where they need a lot of time to reach to the nearest urgent care. Based on [55][55], 20% of US residents live in rural areas and only 9 percent of physicians work there. When wearable sensors enhanced by remote health monitoring, it brings the possibilities on reaching long distance patients and provide them the healthcare they need with low expenses.

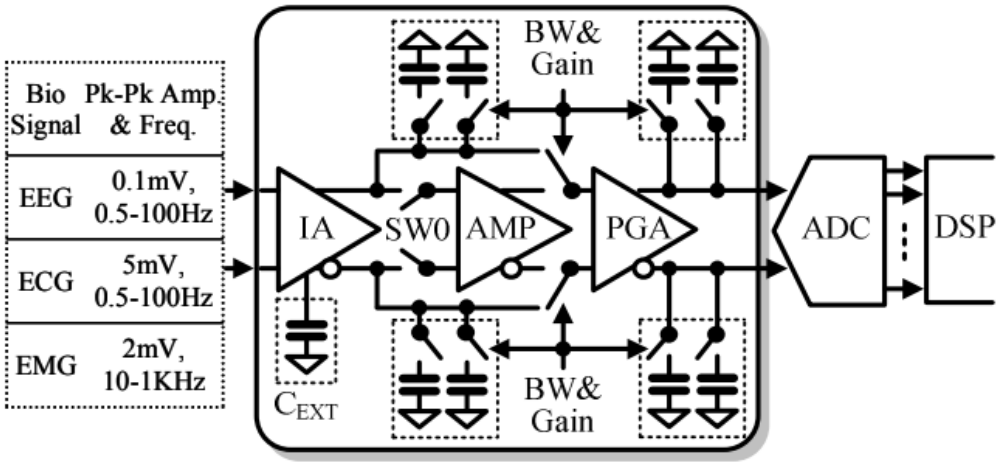

Figure 2. 2: IC architecture of multiple biomedical signal aquistion [68].

2.3 3D-printed Electronics

Additive Manufacturing (AM) is of tremendous interest for rapid prototyping in applications of product development, manufacturing aids, architecture and bio-inspired medical devices. It is used for visualizing conceptual models of actual complex products that further helps avoiding critical design errors or inspire a better product design. Moreover, it is used to fabricate customized prosthetics, and implants. In electronics industry, 3D printing has gain significant attention due to the possibility of massive production of electronics in wide range of applications including wearable biomedical devices. The advancement on this research field could complements the conventional electronics fabrication that is based on silicon [6].

In [12], four electrically small antennas were constructed on 3D surfaces. In which a concentrated silver nanoparticle ink pattern onto surface of hollow glass hemisphere. Unique embedded 3D-printing method is developed [69] using conductive ink and can be applied for sensitive and flexible strain sensor to detect multiple hand gesture. 3D-printed soft robot is reported [70]. The robot is controlled with non-traditional method by fabricating soft materials that is controlled by microfluidic logic. In [71], Fabrication of 3D-printed stretchable piezoresistive sensor is demonstrated.

Ag/AgCl electrodes were utilized in a wireless EEG system for daily healthcare monitoring [56]. Elastomer poly was used to develop a novel polymeric dry electrode and was compared with Ag/AgCl [58]. The test measurement was on detecting and monitoring ECG signal for several days. Comparison between wet, dry and insulating electrodes has been shown in [59]. It shows a development of electrode-skin isolation by dielectric material. However, these electrodes increase the effect of motion artifacts and noise levels [60]. 3D printed dry electrodes were designed, fabricated and tested for recording ECG/EEG signals. The experiment results show a possible

substitution of the standard Ag/AgCl type to enhance the patient comfort [61]. Another 3D printed dry electrode has been reported in [62]. It did not reach to the performance of the standard wet electrode but it produces a usable signal and with some design modification it has the capability to accommodate a gel for better performance. Hydrophobic electrodes made of carbon black powder and polydimethylsiloxane was developed and tested underwater [63]. It can be used for heart monitoring of scuba divers. Some of these electrodes are shown in figure 2.2. Table 2.1 shows a summary of the most recent utilized electrodes with intended applications.

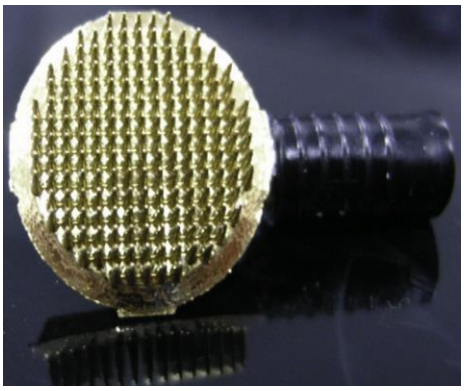

3D printed dry electrodes consisting of 180 conical needles (Titanium Gold)

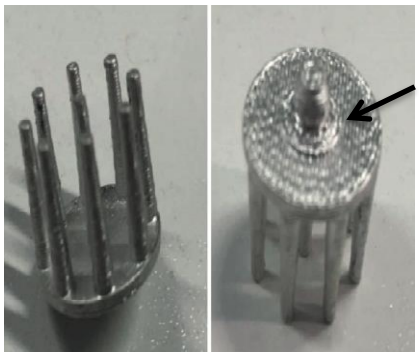

3D printed dry electrodes coated with silver

Hydrophobic electrodes for underwater ECG monitoring

Figure 2. 3: 3D-printed bio sensors.

Table 2. 1: Comparison with some related work

Reference	Measured signal	Type of sensor	Applications
[25]	EEG	Electrodes on scalp's surface	Controlling home appliances
[26]	EEG	16-Channel EEG Cap	P300-based BCI
[29]	EEG	Dry electrode on frontal loop	Students attention level in classroom
[30]	EEG	10-20 standard electrode position system	Emotion classification
[31]	ECG	Standard electrodes on chest	Health monitoring
[33]	ECG	NA	ECG monitoring
[35]	ECG	Wrist-worn device	Portable health monitoring
[37]	ECG	Standard electrodes on chest	Monitoring system for space and terrestrial
[51]	ECG	Standard electrodes on chest	Self-test heart attack
[64]	EEG-ECG-EMG	NA	To prevent sudden unexpected death in epilepsy (SUDEP)
[56]	EEG	Active electrodes	Daily healthcare monitoring
[65]	ECG	Sensors on steering wheel	ECG monitoring in vehicles
[66]	ECG	Active dry electrodes	Monitoring device
[67]	EEG-ECG-EMG	Fabric-embedded electrodes	Health monitoring/Controlling smart home devices

2.4 Physical Vapor Deposition

There are several deposition techniques for depositin metal films on semiconductor wafer such as, Electrochemical Deposition, Chemical Vapor Deposition (CVD), and Physical Vapor Deposition (PVD). In this dissertation, PVD was mostly used to achieve highly conductive interconnects as replacement to the utilized conductive incks in 3D-printed microsystems. That includes two main types of PVD, a) evaporation and, b) sputtering.

Evaporation is performed in a high vaccum to avoid collision with environmental gas molecules in the chamber which might cause contamination. Therefore, very low champer pressure (typically 10^{-6} torr) is important to increase the mean free path. The mean free path is given by [74]:

$$\lambda = \frac{\mathrm{kT}}{\sqrt{2}\pi P d^2},$$

where k is poltsman constant, T is absolute temperature of the champer, d is gas molecule diameter and P is the pressure. In the developed 3D-printed microsystem, e-beam evaporation is used to perform uniform and direct thin film deposition. Sputtering used to perform better step coverage that is needed in the bottom layer of the developed microsystem.

Chapter 3 Wearable Fabric-embedded IEM

3.1 Introduction

In this chapter, investigation of research unique aspects for integration EEG/ECG/EMG lightweight wearable microsystem (IEM) is presented. Available devices and technology related to IEM are explored. Design and preliminary results of bio-signal detection device is demonstrated showing problems encountered with initial-IEM.

3.2 Exploration of off-the-shelf devices

There are several bio signal devices related to IEM are available in the market:

- MG-300 module is capable of detecting EEG/ECG/EMG but it lacks simultaneous measurements of these bio signal. The importance of detecting EEG/ECG/EMG continuously and at the same time is reported in 2017 [64] for help preventing sudden unexpected death in epilepsy. In order to use MG-300 as IEM, it requires three modules which is highly not desired for lightweight wearable devices.
- MyoWare sensor is designed for detecting and measuring the electrical activity of muscles (EMG). This sensor can be applicable in many smart home devices such as switching ON/OFF appliances through muscle contraction and stretching.
- NeuroSky device is used for measuring the electrical activity of the brain (EEG). It is capable of detecting the EEG power spectrum and separating each frequency range of a brain signal to be implemented in many applications including sleeping monitoring.

If all these devices are embedded inside clothes, it is expected to be very demanding by many industries, especially in smart homes and health monitoring applications (Fig. 3.1). Therefore, this work is focused on producing preliminary results for IEM and then develop an innovative technique for fabric-embedded IEM.

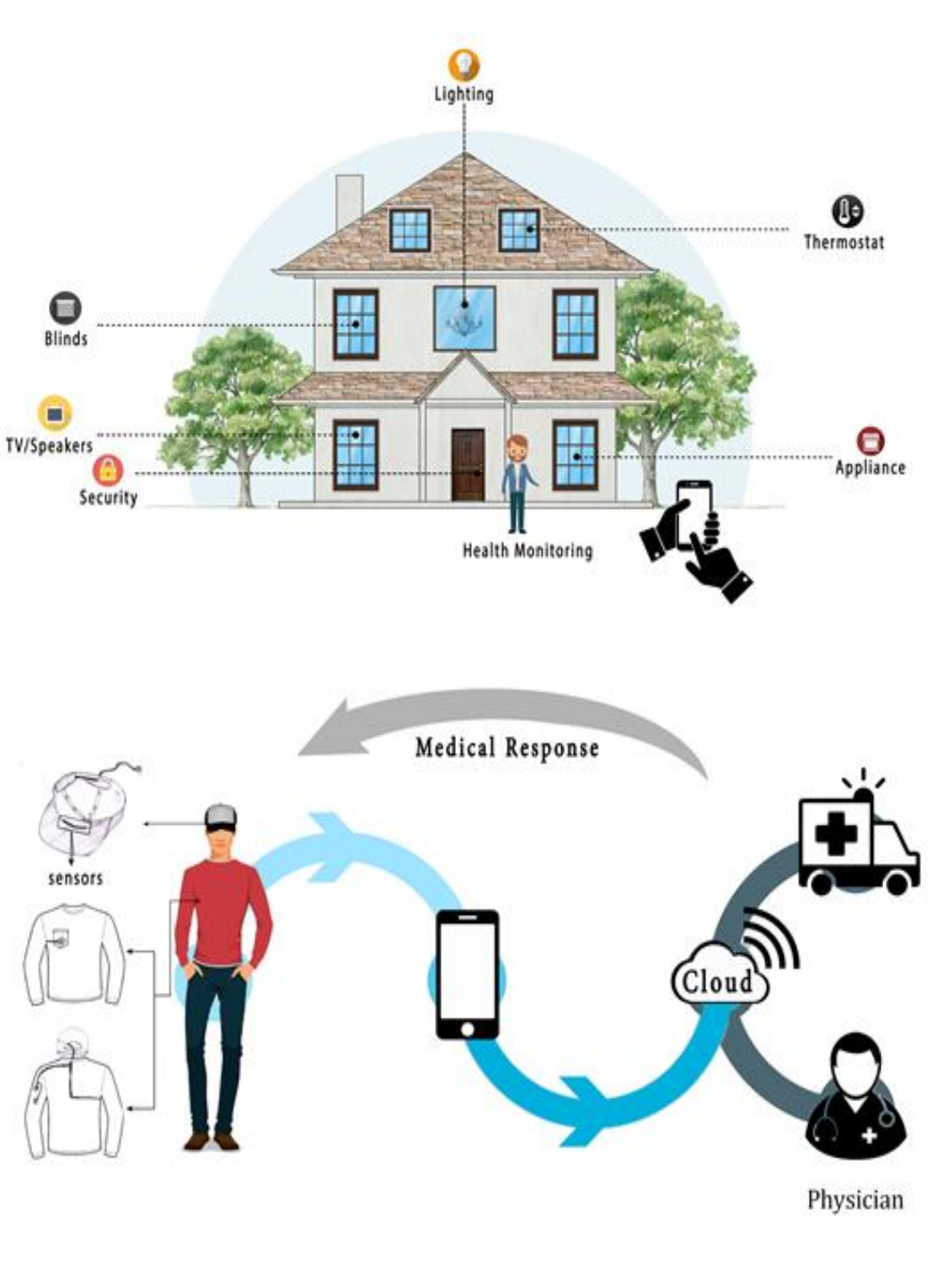

Figure 3. 1: Conceptual diagram of fabric-embedded IEM, objective and possible applications.

A)

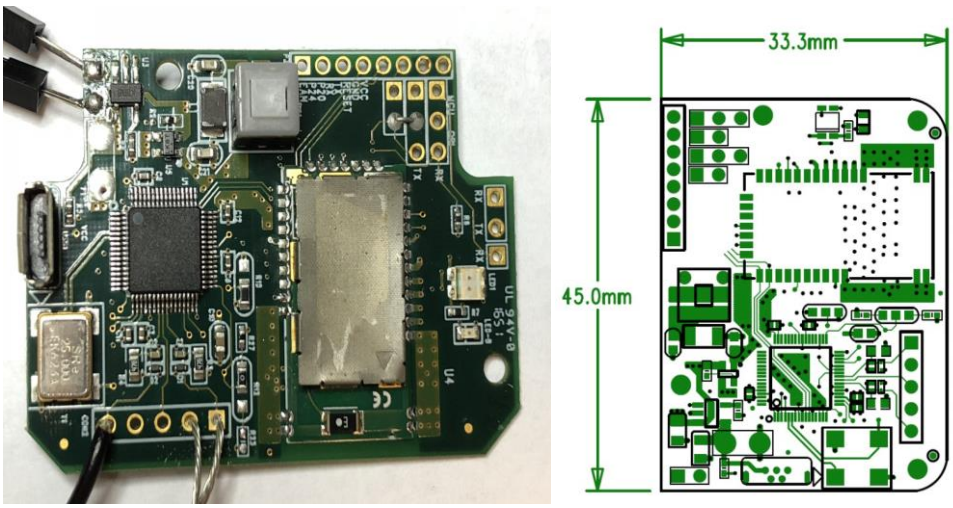

B)

C)

Figure 3. 2: off-the-shelf biomedical signal acquisition devices: A) MG-300, B) Mindwave mobile from NuroSky, and C) MyoWare sensoe from Advancer Technologies.

3.3 Initial study and experiments of IEM

This section will summarize the fundamental knowledge needed to design and implement a bio-signal detection. In particular, the targeted bio signals are EEG, ECG and EMG. The methodology followed in this study was in determining the measurement requirements of each bio signal and the basic block of each stage of the signal conditioning module.

3.3.1 Design Parameters

Each bio-signal has different characteristics in nature and therefore, they require unique circuit design to be detected properly. For example, EEG signal demands much more amplification than ECG or EMG due to its weak amplitude (10 uV). In addition, the half power frequency of the EEG is different than ECG and EMG. Which requires different filter design for each bio signal measurement. Table 2 below summarizes the design requirements of each stage of the schematic. That includes the total gain amplification and cutoff frequencies of all filters of IEM.

Table 3. 1: Design Specification of IEM

Bio-signal	Amplifier Gain	High pass filter (Fc)	Low pass filter (G/Fc)	Notch filter (G/Fc)	Total Gain
EEG	58	0.16Hz	31/62Hz	1/60Hz	19778
ECG	6	0.16Hz	6/100Hz	1/60Hz	396
EMG	11	10Hz	8/1kHz	1/60Hz	968

3.3.2 Schematic Design

The signal conditioning design consists of several stages as shown in the block diagram in Fig. 3.2. It starts with sensors that detect the signal from the surface of the skin and then to instrumentation amplifier through twisted pair wire for noise cancellation and reduction. Then it introduced to the filter stages where the signal will be classified based on frequency ranges. Because the utilized battery is the regular 9V, a regulator and rail splitter is needed for IC's biasing. The Instrumentation Amplifier (IA) amplifies the difference between two input signals and rejects the common noise signals. Therefore, a high common mode rejection ratio is necessary in the application of bio signals to increase the noise immunity of the design. Due to the weakness of the bio signal, any small noises could be very harmful to the signal. In addition, the two input wires need to be very close to each other to ensure same noises affecting the two inputs.

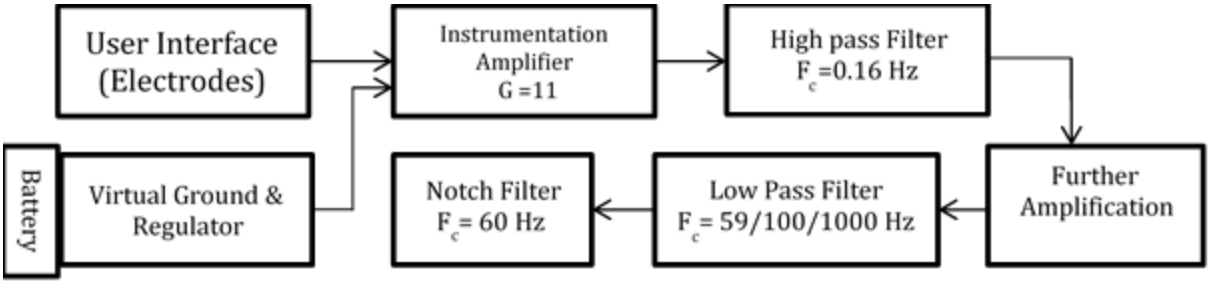

Figure 3. 3: Block diagram of the analog module of IEM.

3.3.3 Filters

The stage of filters is tremendously important when dealing with low power signal such as the EEG. It can be easily conquered by noises and it is challenging to eliminate these noises without harming the desired signal. A passive high pass filter for DC blocking is used with cutoff frequency of 0.16Hz. Moreover, two main active filters were implemented for low pass and notch filter.

- **Active Low Pass Filter**

In addition to the passive filter, low pass filter is used to attenuate the undesired high frequency ranges. In the case of EEG, the -3dB bandwidth of the amplifier was set at 59 Hz whereas in the ECG design, it was at 100Hz. The frequency range of the EMG signal is much higher than the previously mentioned bio signals. It starts from 10 Hz to 1 kHz. Therefore, the cutoff frequency of its low pass filter was set at 1000Hz.

- **Active Notch Filter**

The notch filter is a special type of the band-stop filter. It eliminates a very narrow frequency band. The importance of the notch filter in the initial design of IEM was in rejecting noise of the line interference at 60Hz. A twin-T network that consists of a parallel connection of a low pass filter and high pass filter were utilized. The feedback resistor was calculated to be 1kohm but with practical testing tuned using a potentiometer to 1160 ohm.

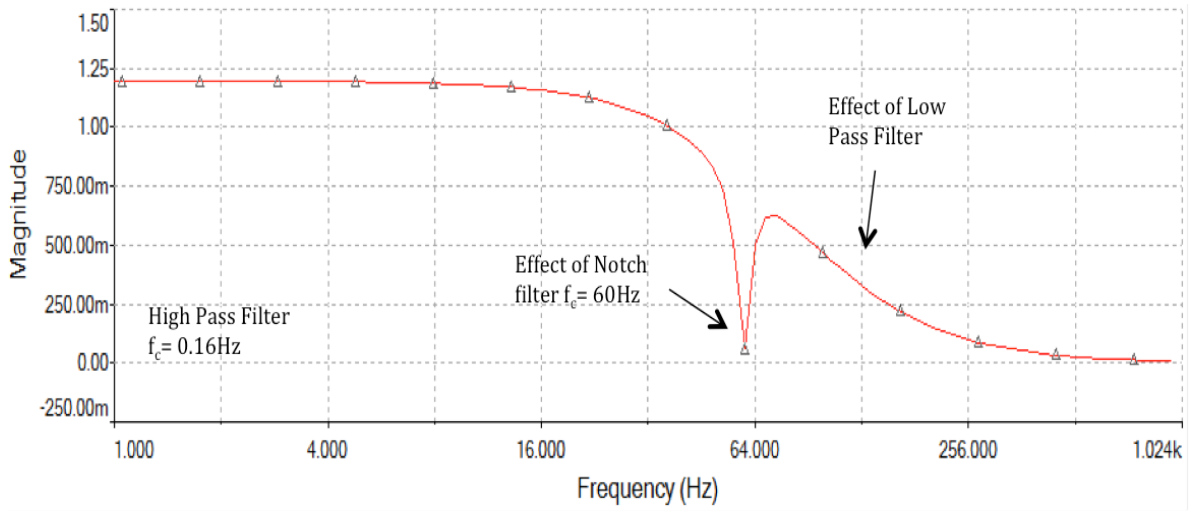

Figure 3. 4: Frequency response of high pass filter, low Pass filter and notch filter.

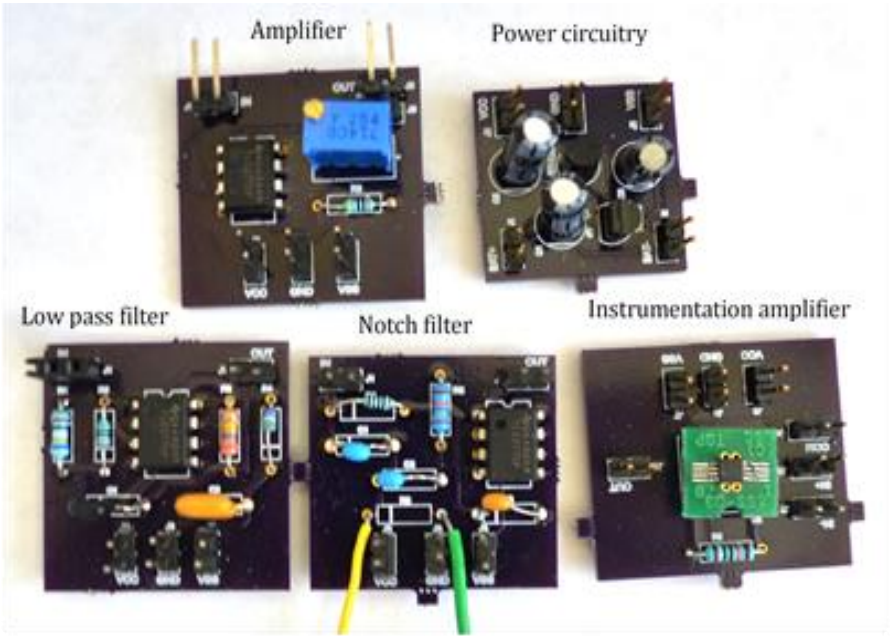

Figure 3. 5: Mini-PCB's design for initial test of IEM's components.

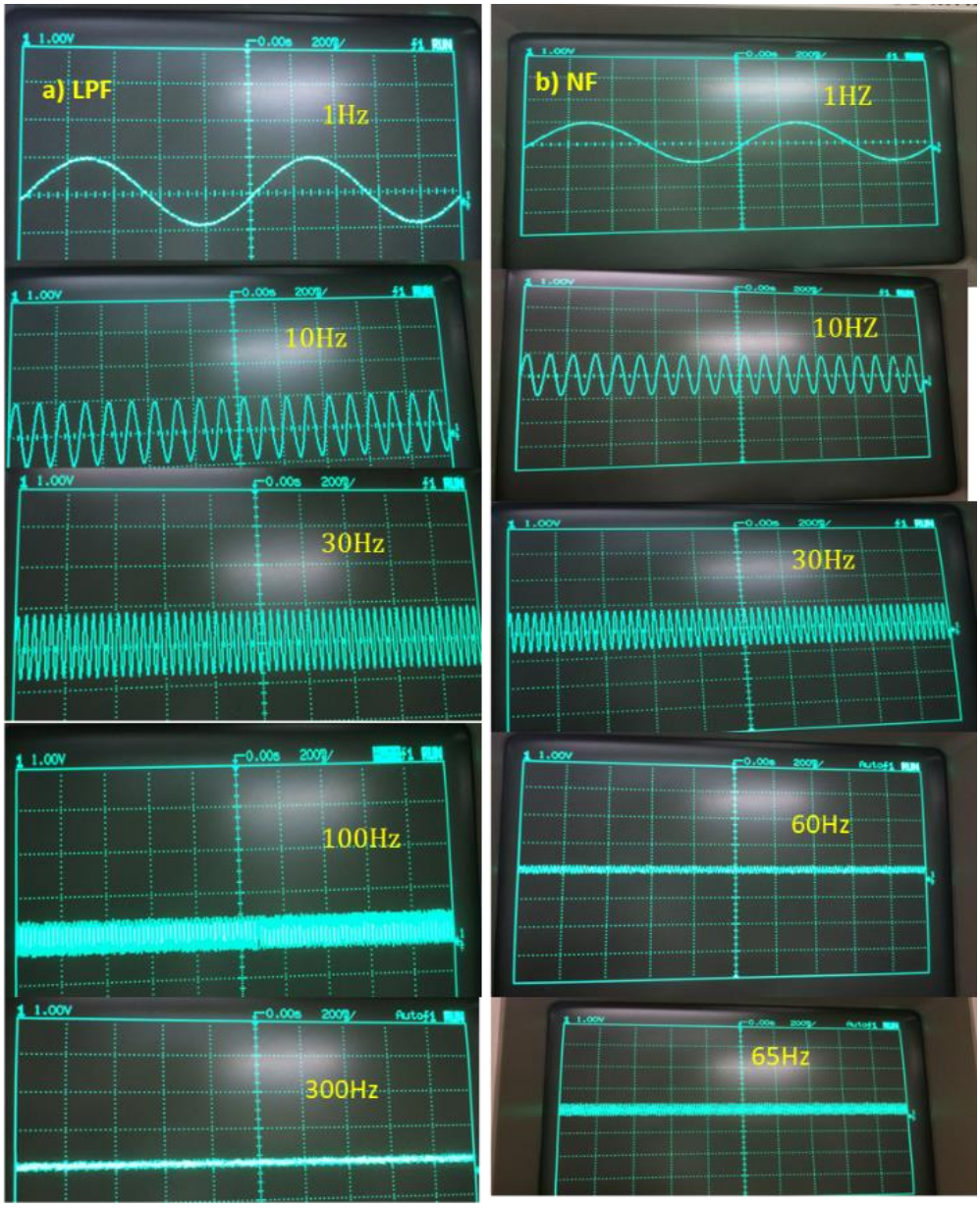

Figure 3. 6: Tested frequency responses of a) low pass filter (LPF), and b) notch filter (NF).

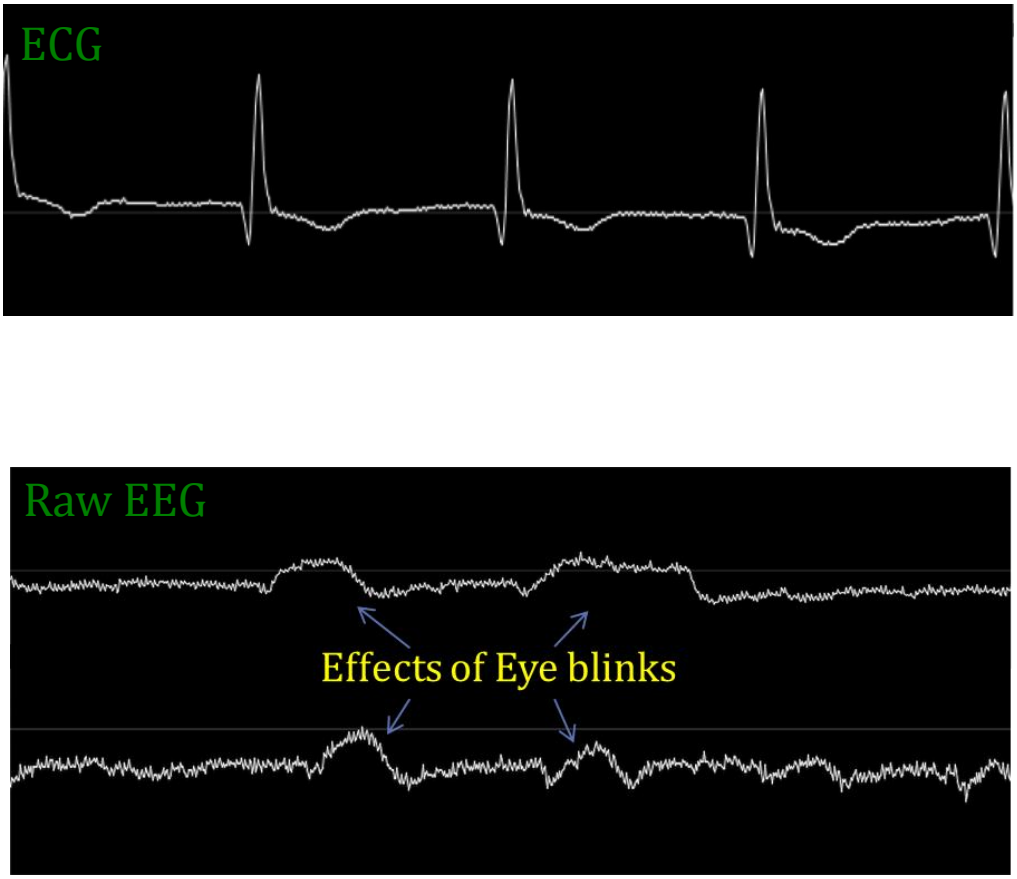

Figure 3. 7: Results of separate PCB for ECG and EEG bio-signal acquisition.

3.3.4 Power Management

For initial design of bio-signal detection, a single 9V battery can be utilized to supply all the active stages of the bio signal schematic. If the biasing voltage is for example ±2.5, then LM78L05 regulator can be used to step down the input voltage to 5V and followed by a virtual ground circuitry (rail splitter) to split the voltage to ±2.5V. TLE2426 is a suitable option for that purpose due to its very high precision.

3.3.5 IEM Schematic

The generic full schematic of the design is shown in fig. 3.6. Instrumentation amplifier was first interfaced with the dry electrodes due to its high noise immunization. Then the stage of the DC blocking placed. After attenuating most of the noises with low gain, further amplification using multi-turn trim potentiometer was provided. Then it was cascaded with two main active filters, the low pass filter and the notch filter. The gain amplification was split to all stages starting with lowest gain provided in the first stage to avoid further noise amplification and to further controlled gain in later stages.

3.3.6 Issues

There are some issues encountered the initial design of IEM as listed below:

- The output resulted in the single PCB, Fig. 3.8, were not as accurate as the one detected with the sperate PCB design Fig. 3.5. The reason for that is noise created by the large amount of component in the single PCB.
- The power consumption of the PCB is quite large due to the number of IC's used. It will be very sophisticated if the renewable energy, such as solar/kinetic, can be integrated with the system.
- Noise shielding was not implemented which could highly affected the testing results.
- The weight and dimensions of IEM is considered large as a wearable device and need to be miniaturized. Therefore, utilizing single chip consisting all the required main schematic stages would highly desired for realizing multifunction lightweight microsystems.

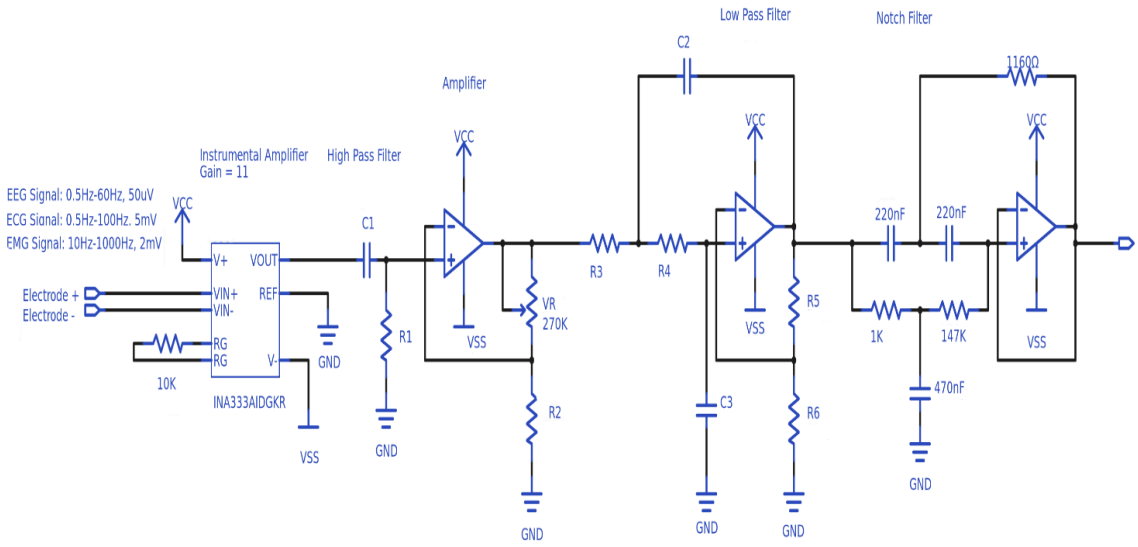

Figure 3. 8: Initial Schematic design of IEM.

Table 3. 2: List of passive components.

Parameter	C1(F)	C2(F)	C3(F)	R1(Ω)	R2(Ω)	R3(Ω)	R4(Ω)	R5(Ω)	R6(Ω)
EEG	1μ	180n	2.2μ	1M	4.7k	3.3k	5k	226k	7.5k
ECG	1μ	180n	2.2μ	1M	54.9k	649	10k	270k	54.9k
EMG	100n	22n	10n	150k	27k	4.2k	24k	226k	32k

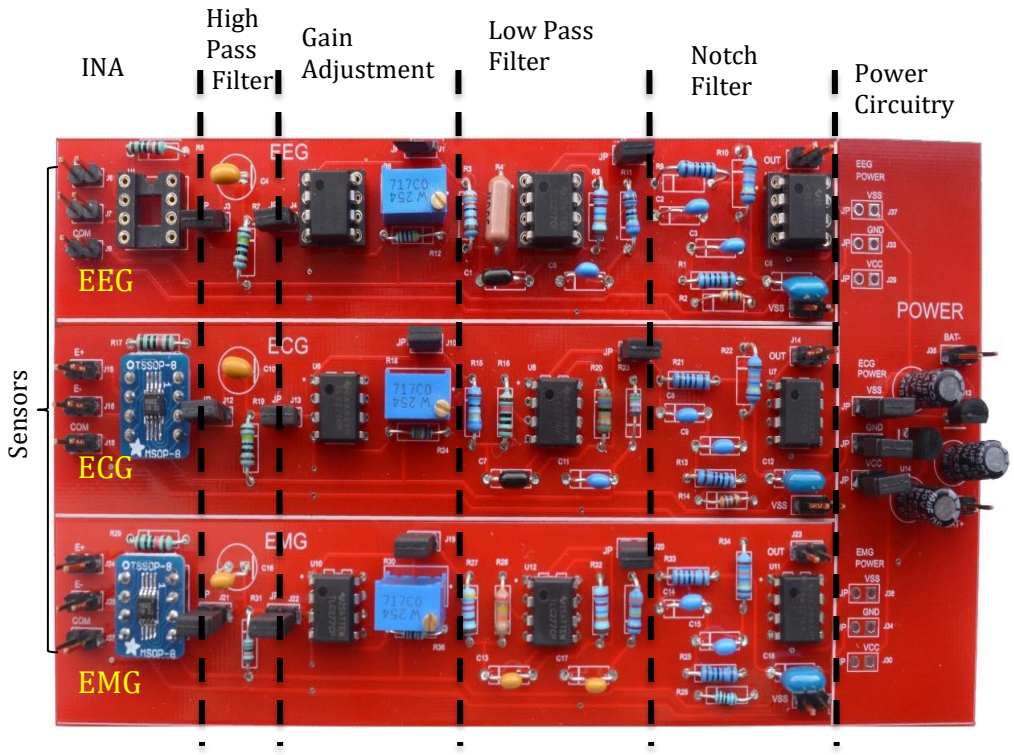

Figure 3. 9: Picture of the single PCB design of IEM.

3.4 Miniaturization for fabric-embedded 3D-printed microsystem

Due to the issues encountered in the initial experiments of IEM and because of the complexity of 3D-printed microsystem processes (presented in chapter 4 and 5), it is determined to limit the design to ECG and EEG microsystems separately. Therefore, the focus of the work is directed toward the innovative design of fabric-embedded microsystem. The rapid production, variety of materials and the wide range of application of 3D printing makes it a substantial opportunity for novel and innovative ideas. This work can easily be extended for EMG and EEG microsystem.

It is necessary to implement miniaturized microsystem for better demonstration of 3D-printed microsystem processes. Therefore, single chip (AD8232) consisting of instrumentation amplifier, buffer reference and operational amplifier will be utilized. The chip is developed by analog devices for heart monitoring. The utilized schematic of 3D-printed microsystem is shown in Fig. 3.9. In order to utilize the chip for EEG signal acquisition, several critical design issues need to considered. The input voltage is very low and requires low offset voltage (<< 10 uV). The device characterization is shown in table. 3.3. In the EEG circuit design, the average gain is 79.5 dB with potentiometer set at 97k Ohm. The first stage gain can be adjusted by:

$$\frac{R1 + R3}{\mathrm{R2} + \mathrm{Pot}} + 1$$

Total CMRR is 80dB which is determined by the internal instrumentation amplifier of AD8232. The input resistance is very high and determined by input resistance of TLV333. The right leg driving circuit helps reducing the common mode noise allowing CMRR to increase to 116 dB. The current consumption is 200 μA at 2.5V.

Table 3. 3: Device charectrization for EEG and ECG signal acqusition

Parameters	**EEG**	**ECG**
Input voltage range	60 µV	5 mV
Measurent tolerance	5µV	100 µV
Differential impedence	100 MOhm	100 MOhm
CMRR	100dB min	80dB
GAIN	10000	500
Supply voltage	3V CR2032	3V CR2032

A)

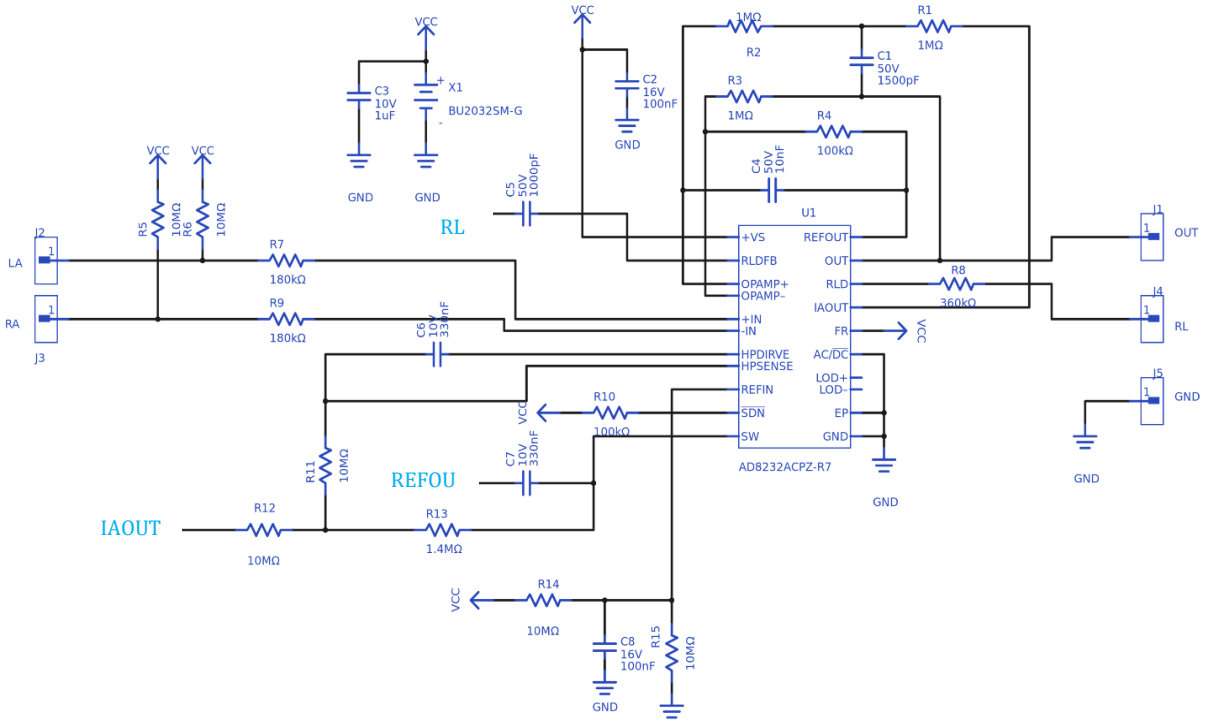

B)

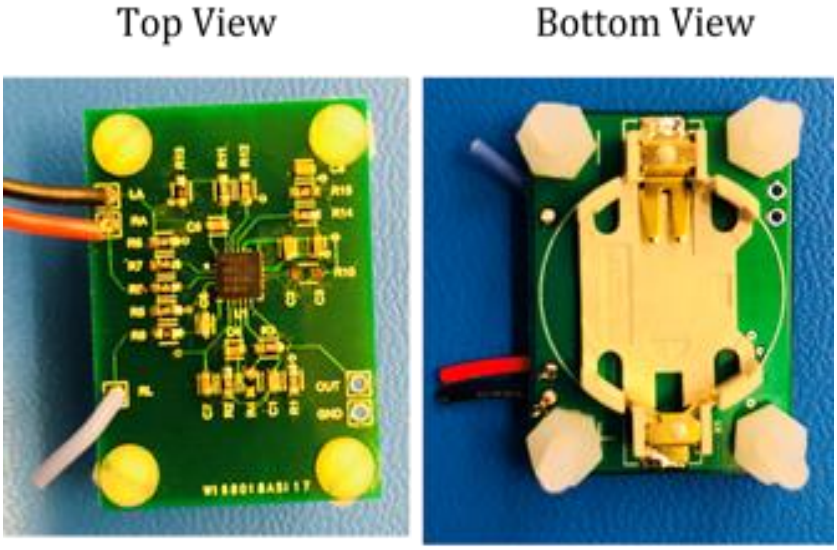

Figure 3. 10: A) Schematic design and B) Conventional microsystem for ECG using AD8232

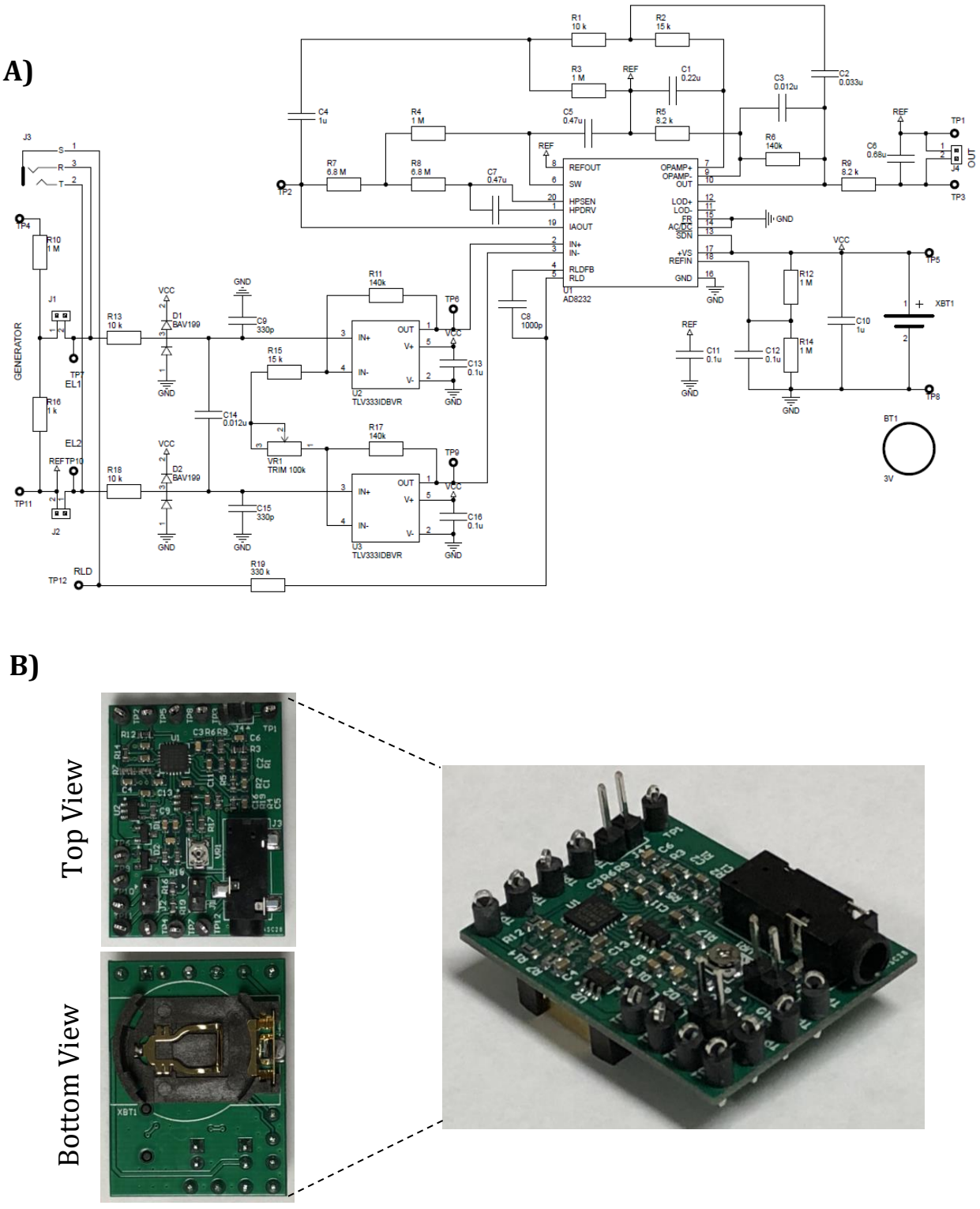

Figure 3. 11: A) Schematic design and B) Conventional microsystem for EEG using AD8232 .

Chapter 4 3D-printed Microsystem Processes

4.1 Introduction

The current main issue of 3D-printed electronics is the high resistivity of conductive inks which requires curing at very high temperature. The substrate of the 3D-printed microsystem can barely handle 100 degree-celsius befor it reach its melting point. The minimum resistivity reached in 2019 [75] is 98 μΩ with silver-based conductive ink. This is still far away from the bulk resistivity of the copper film (1.67 μΩ). Another issue of the conductive ink is that it consist of many components which makes very expensive. 115g of silver conductive ink cost $295 (MG Chemicals). Finally, the conductive ink suffers short life at room temperature. Aged conductive ink (7 days) shows 5% higher resistivity than as printed conductive ink [15].

In this chapter, new patterning process for three-dimensional 3D multilayer microsystem is implemented from scratch to final product. Starting from fabricating simple isolated metal interconnects to establish novel process technology, ECG test microsystem were designed and fabricated. This demonstration shows the capabilities of additive manufacturing in the future electronics industry.

4.2 New Selective Deposition Method

This section deals with the patterning technique utilized in this work for selective metal deposition of isolated interconnects in a microsystem. It presents a 3D-printed design of a shadow mask with designated cavity and self-alignment for thin film deposition. In addition, it includes the major difficulties and challenges with the proposed solutions.

Since the major filaments of conventional 3D printers are plastic-based material, it is necessary to identify the most suitable method for selectively depositing metal films with good adhesion quality suitable for these filaments.

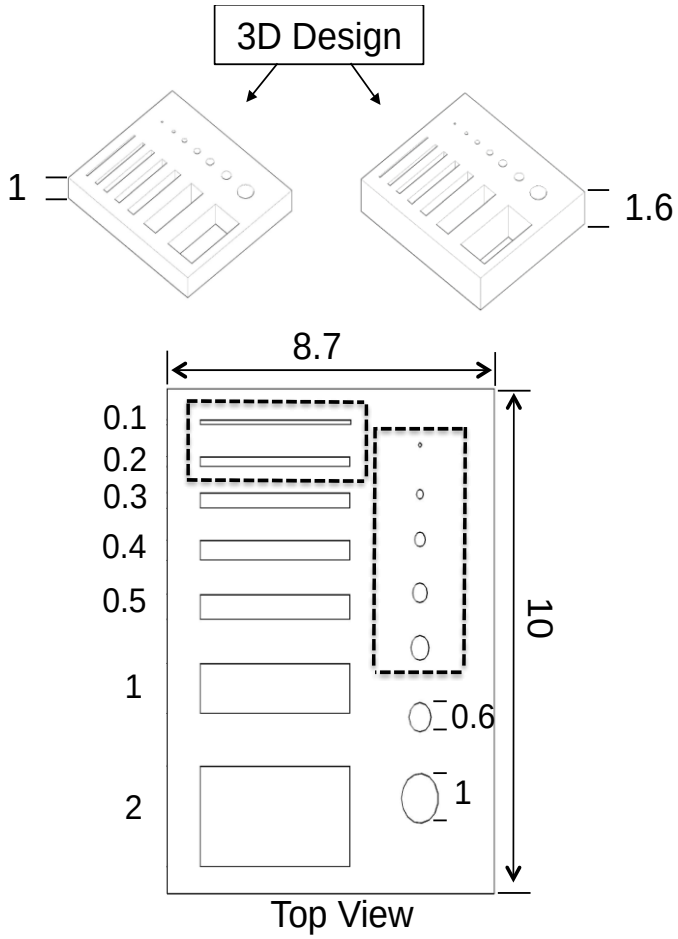

Dashed boxes are for non-printed dimensions. Either totally blocked or not well penetrated

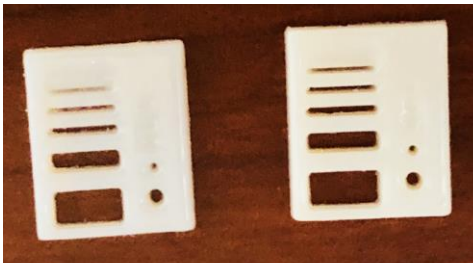

3D printed Structure

Figure 4. 1: Testing resolution of the 3D-printer, all dimensions are in mm unit.

The basic component used in this chapter for implementation of 3D-printed microsystem includes three major steps:

1) Computer Aided Design
2) 3D Printed Structures
3) Metallization

All the printed structures were designed using AutoCAD software and printed with the Object Connex 350. In the beginning of the design, it is necessary to identify the resolutions of the utilized 3D printer to initiate proper dimension of the first implemented microsystem. Therefore, a tested design with different dimensions of apertures of rectangular and hole shapes was implemented as shown in Fig. 4.1. Al the printed samples were cleaned with distilled water and rinsed with Nitrogen. For process implementation on single substrate, four structures were designed and printed: 1) shadow mask, 2) substrate, 3) electroplating frame, and 4) holder. These components designed to fit through in top layer and pillars in bottom layer for self-alignment.

4.2.1 Self-aligned Shadow Mask

In the design of 3D-printed microsystem, several issues were investigated including printer resolution, vertical interconnect access (via), patterning of conductive interconnects, adhesion and electroplating process. The key part in this technology is a plastic-based self-aligned shadow mask with designated cavity that allows evaporated metal particles to pass through and stick on the substrate layer to create selective deposition of thin films of broader types of metal target including Cu, Au and Ni. This approach provides metal interconnects on plastic substrate more efficiently than conductive inks for the following reasons: a) no curing, and b) low resistivity interconnect. Fig. 4.2, shows a concept diagram of shadow mask (a-top) with cavity shaping conductive patterns

that is accomplished through Physical Vapor Deposition (PVD) and thin layer printed substrate (a-bottom) prior to metal deposition.

The minimum aperture for traces width and hole diameter using the Connex 350 was found to be 0.3 mm and 0.6 mm, respectively. Advanced development in printing machines with higher resolutions will lead to smaller aperture dimensions as close as conventional CNC routing in printed circuit board. After optimizing the samples dimensions, the structures were printed and rinsed with DI water. Then heat processing and plasma treatment were performed to degas and further clean the samples from contamination prior to deposition process. Each inner layer of the microsystem is implemented with same procedure as in the top layer.

4.2.2 Vertical Interconnect Access (VIA)

There are several possible ways to achieve electrical connection between microsystem layers in the vertical direction by utilizing the ability of the 3D printers. One way is to design separate connection that after metallization can be snapped in the bottom of the top layer as shown in Fig. 4.3.

In this work, via is approached through extruded pillars to provide electrical connection to upper layers of the microsystem, Fig. 4.2b.

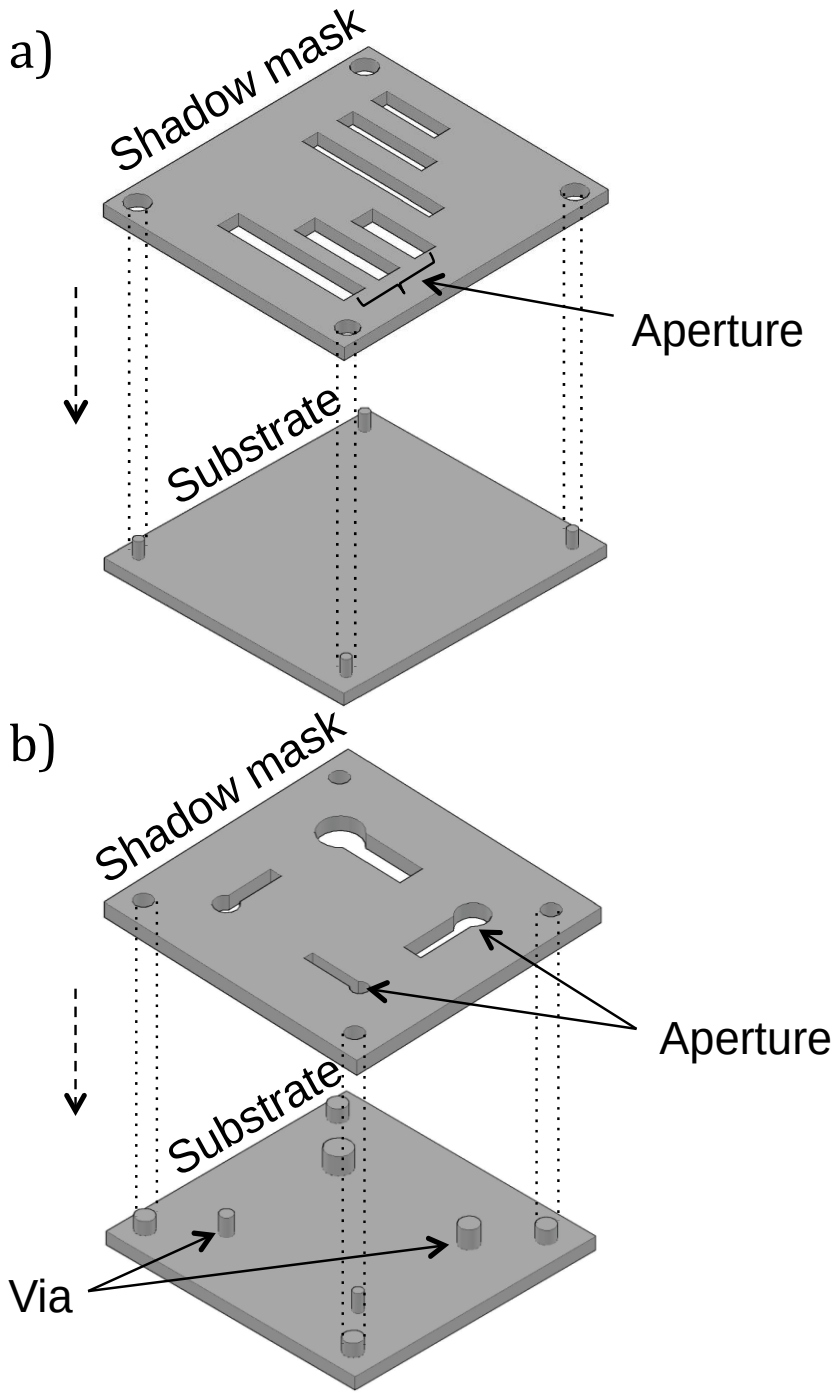

Figure 4. 2: Concept diagram showing method for patterning of a) metal interconnects for top layer and b) vertical interconnect access for bottom layer.

4.2.3 Electroplating Process

As the evaporated films are typically 500 nm thick, they need to be electroplated to increase their thickness in the range of 10 μm. Since in a typical microsystem, the conductive interconnects consist of isolated segments in each layer, these segments need to be temporary electrically connected during the electroplating process. The structure was first designed and printed with extruded knobs and then metalized to create electrical contact to all metalized segments. Diagram of the electroplating setup is shown in Fig. 4.4.

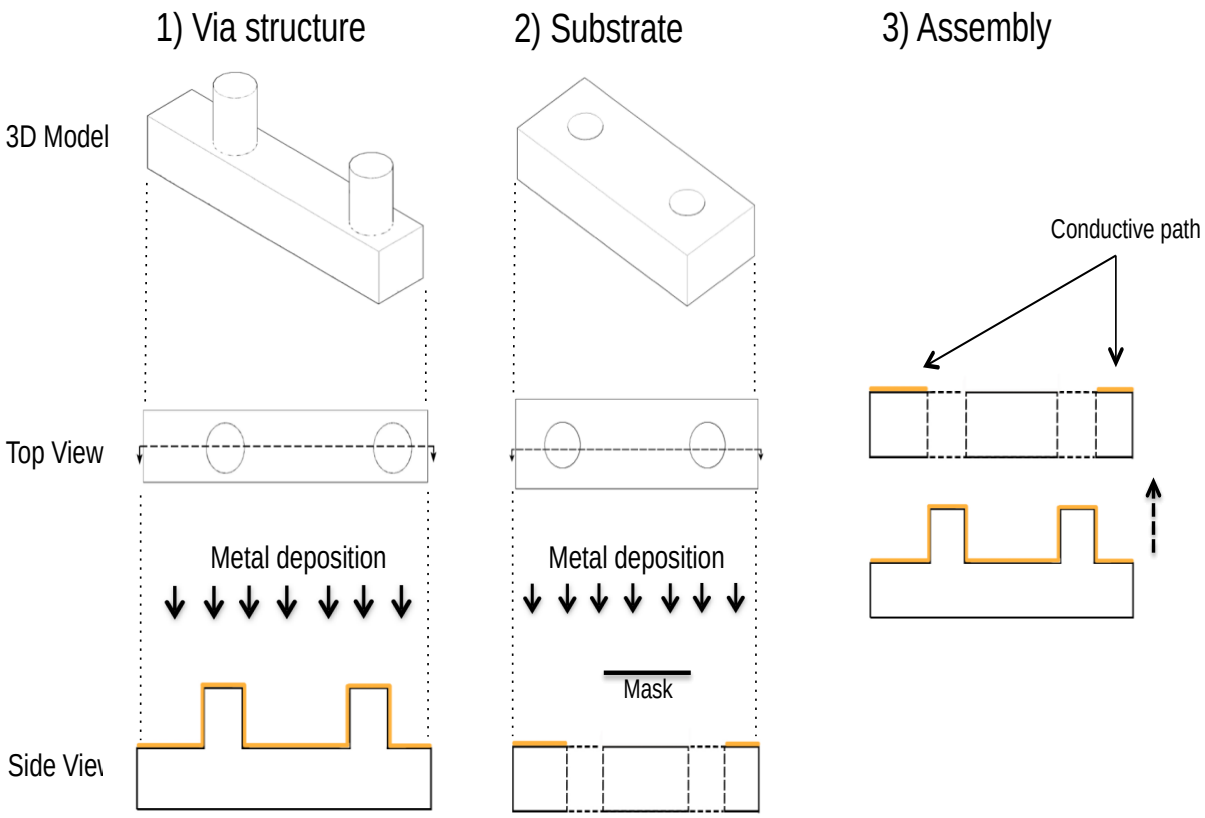

Figure 4. 3: Initial vertical interconnect access (via).

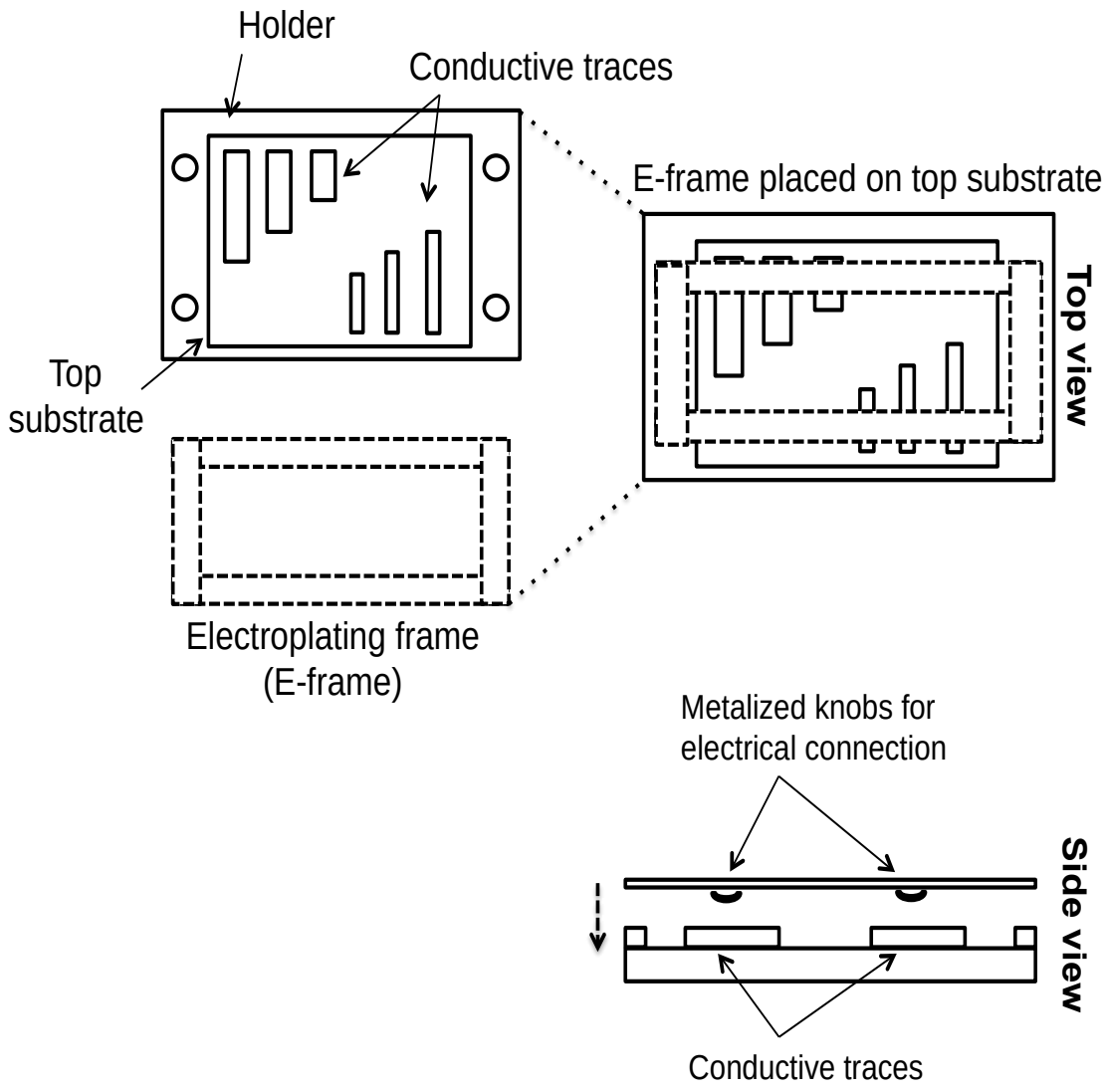

Figure 4. 4: Concept diagram of E-frame (after metalized) attached to all interconnection traces on substrate.

4.3 Metallization

Metal interconnect is an essential portion of any electronic microsystem device. It's highly desired to achieve minimum resistivity in electronic devices for better performance. Furthermore, adhesion between deposited material and substrate is mandatory.

The initial metallization test was conducted through conductive Nickel spray from MG chemicals because it offers high quality adhesive and conductive coating. However, the product did not through small aperture areas that have been created on the printed shadow mask. For comparison reasons, another test was conducted with evaporated copper to identify the differences between nickel spray and physical vapor deposition as shown in Fig. 4.5.

The applied conductive nickel spray created a continuous layer on the apertures below 0.5 mm width, which prevents the deposited material to pass through the shadow mask. In addition, the succeeded deposited material was not forming sharp and uniform edges. When the shadow mask is removed, some of the deposited material was displaced from the substrate. Due to these issues, conductive nickel spray was considered not suitable for 3D-printed microsystem. The initial thought of utilizing this method was to identify the simplest metal deposition that can efficiently implemented in 3D-printed microsystem. Therefore, physical vapor deposition is considered in this work. It offers much better quality and uniformed thin films as shown in Fig. 4.5. The self-aligned shadow mask implemented by designing holes (1mm diameter) and pillars (0.9mm diameter) at the corner of the structures, which allows very precise alignment.

Table 4. 1: Comparison between conductive nickel spray and physical vapor deposition on 3D-printed microsystem

Parameter	**Nickel Spray Deposition**	**Physical Vapor Deposition**
Pattern Sharpness	Poor	Good (e-beam evaporation)
Roughness	Very poor	Good
Adhesion	Good	Good (Ti/Cu)
Conductivity	Good	Very good
Minimum mask aperture	0.5 mm	0.3 mm
Via coverage	Poor	Very good (sputtering)

The proposed process involves three metallization techniques: (1) e-beam evaporation for thin film patterns through the aperture on shadow mask structure, (2) sputtering for step coating of the pillars structures in the bottom layer for interconnecting with top layer, and (3) electroplating for further increasing the thickness of the deposited metal. Two films are deposited:

- 100 nm thick layer of Titanium (Ti) to enhance adhesion between the surface of the substrate and the deposited gold/copper.
- 500 nm thick layer of Gold (Au) when wire bonding is used or Copper (Cu) when soldering used.

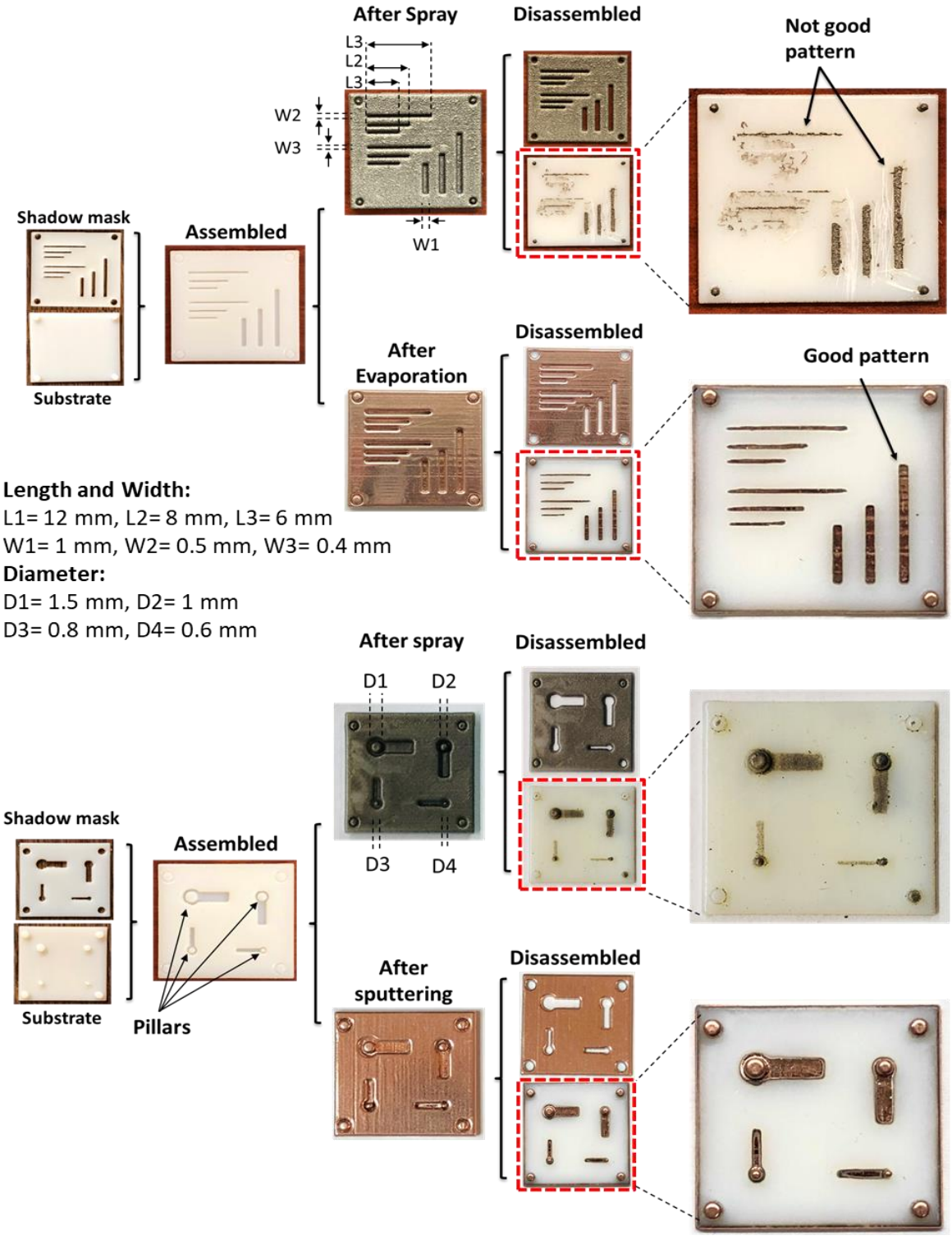

Figure 4. 5: Thin film pattern using conductive nickel spray and e-beam evaporation for, a) interconnects (traces), and b) vertical interconnect access

4.3.1 E-beam Evaporation

The printed samples placed into E-beam deposition chamber with a pressure of $2x10^{-6}$ Torr. Two metal films of 100 nm Ti and 500 nm Au were evaporated on the surface of the sample patterning uniform thin film metal interconnects on the substrate through opening areas on the shadow mask as shown in Fig. 4.6. Since E-beam evaporation is a directional deposition technique, the sidewall (step coverage) that supposed to provide electrical access through inner layers of the microsystem is not fully coated, Fig. 4.7. Therefore, an alternate technique with step coating is needed.

4.3.2 Sputtering

Compared with E-beam evaporated films, sputtering shows a better step coverage on the target substrate. This is critically important for vertical interconnect access through via holes. The shadow mask attached to the substrate and placed into a magnetron sputter deposition chamber. The deposition chamber was evacuated to a pressure of $2x10^{-6}$ Torr; metal films are sputtered on the surface of the sample with 100 nm Ti and 500 nm Au. The source power of Ti target was held at 300W, and for Au target was at 200W, which translated into deposition rates of 1.5 and 7.6 nm/s, respectively. The device showed a good electrical conductivity on different layers. In sputtering, it's highly desired to design the shadow mask accurately and ensure the attachment to the substrate be as close as possible. Because if the shadow mask is not attached to the substrate very well, some of the ejected atoms pass through the shadow mask and creates unwanted deposition. It may also create short circuit between the isolated metal segments.

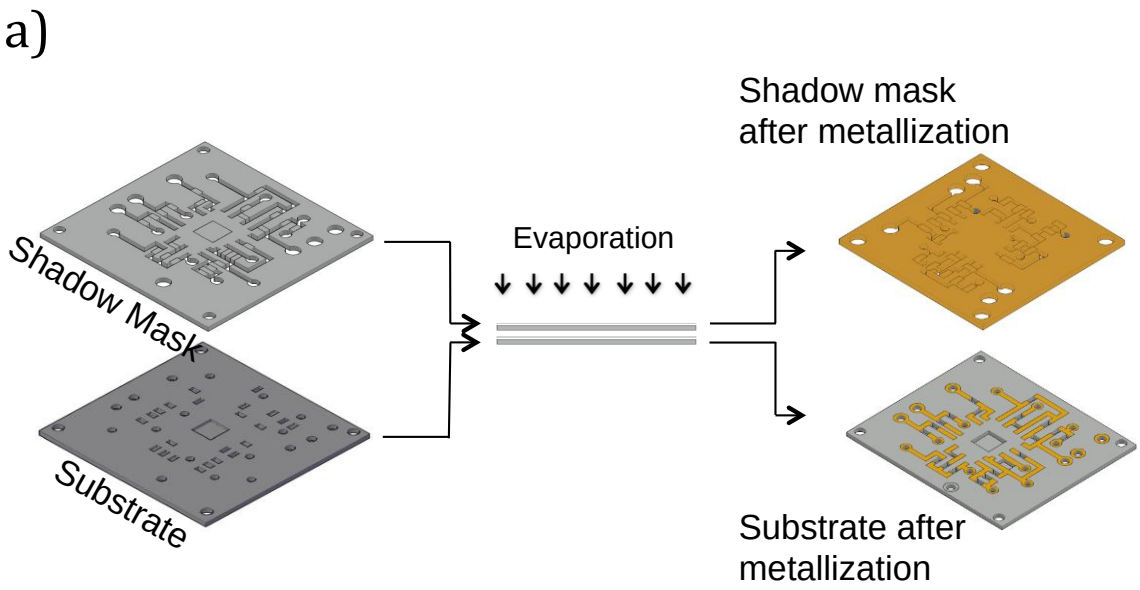

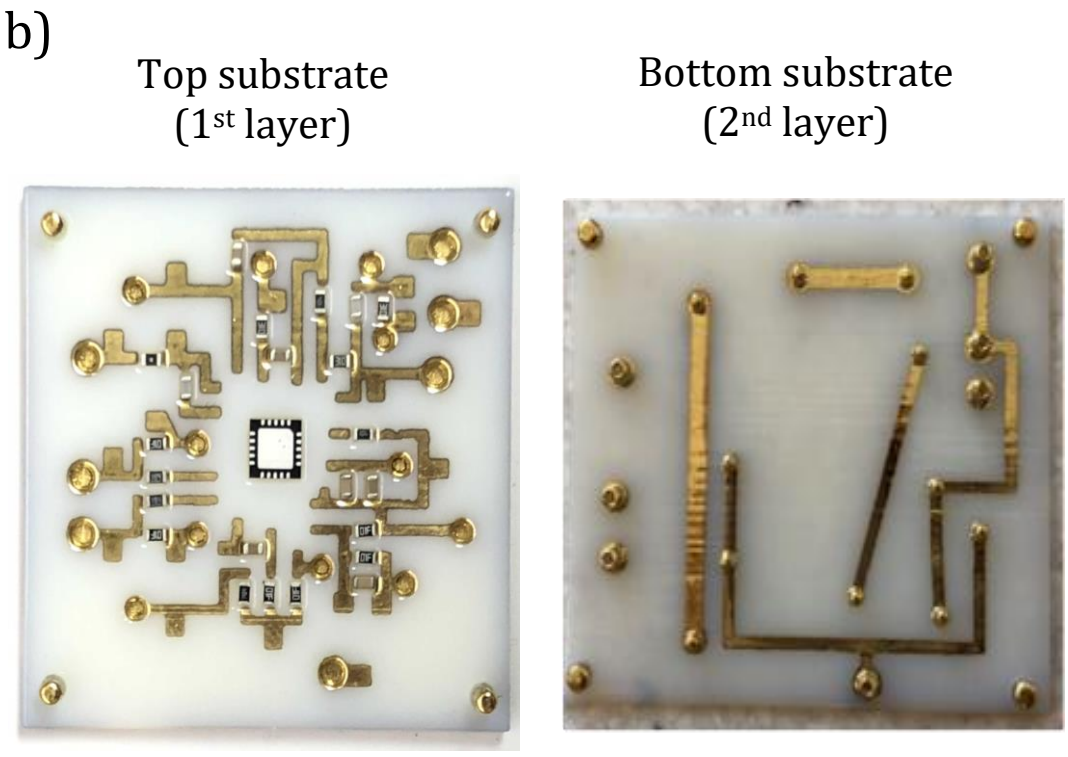

Figure 4. 6: a) Concept diagram of using PVD (e-beam evaporation) on 3D-printed microsystem, and b) real image of the deposited Ti/Au on two layers microsystem.

The thickness of the deposited film is not sufficient for soldering process. While soldering at 50-degree temperature, the deposited film immediately lifts off from the substrate. Therefore, electroplating process is necessary to further increasing the thickness of the deposited layers.

4.3.3 Electroplating Process

For electroplating process, all isolated meal segments have to be temporary connected to a single lead (cathode). Therefore, 3D-printed structure, Electroplating frame (E-frame), designed and printed with knobs touching all deposited thin films on the substrate. Fig. 4.8 depicts the setup for electroplating. The electroplating was successfully implemented achieving 10 microns thick of copper interconnects.

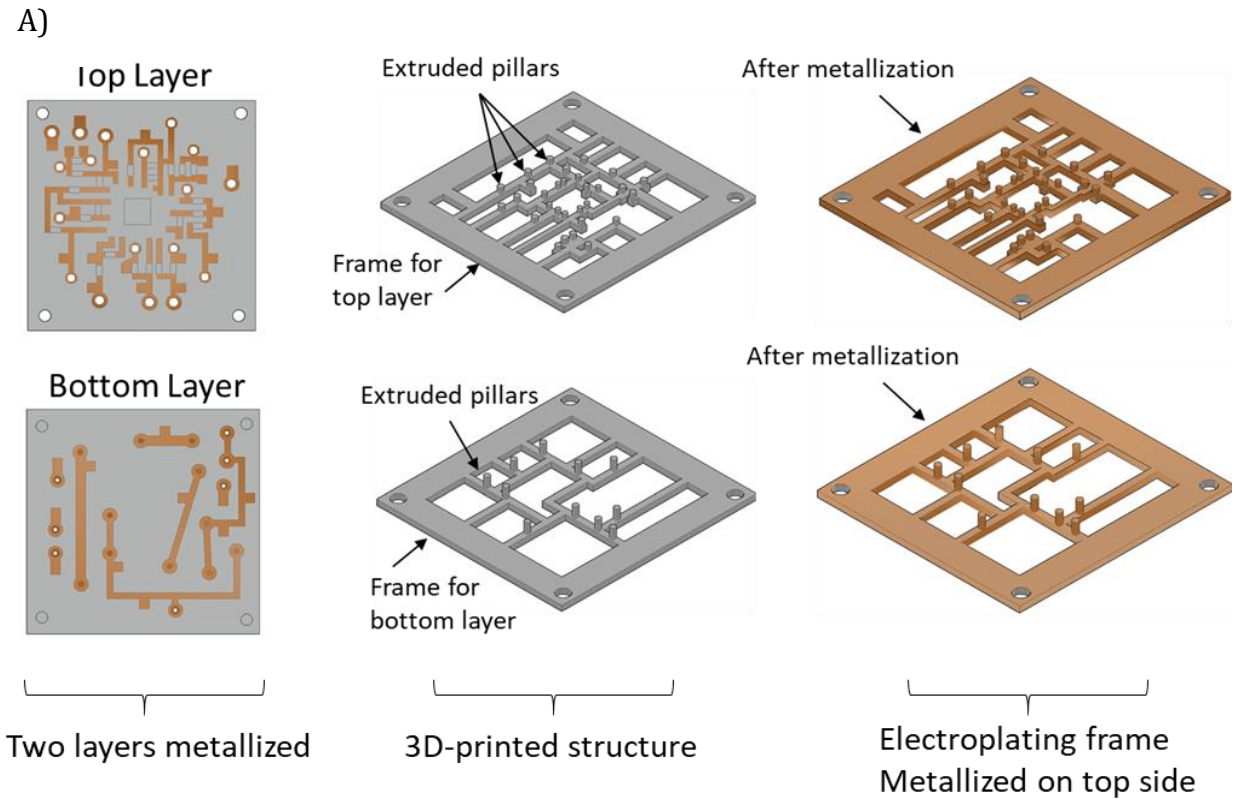

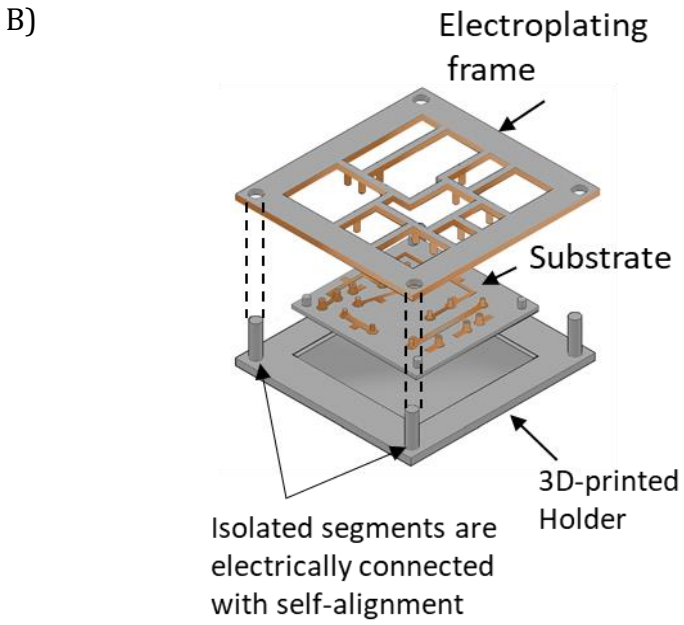

Figure 4. 7: A) Concept diagram of electroplating process on isolated metal segments, and B) electroplating set-up.

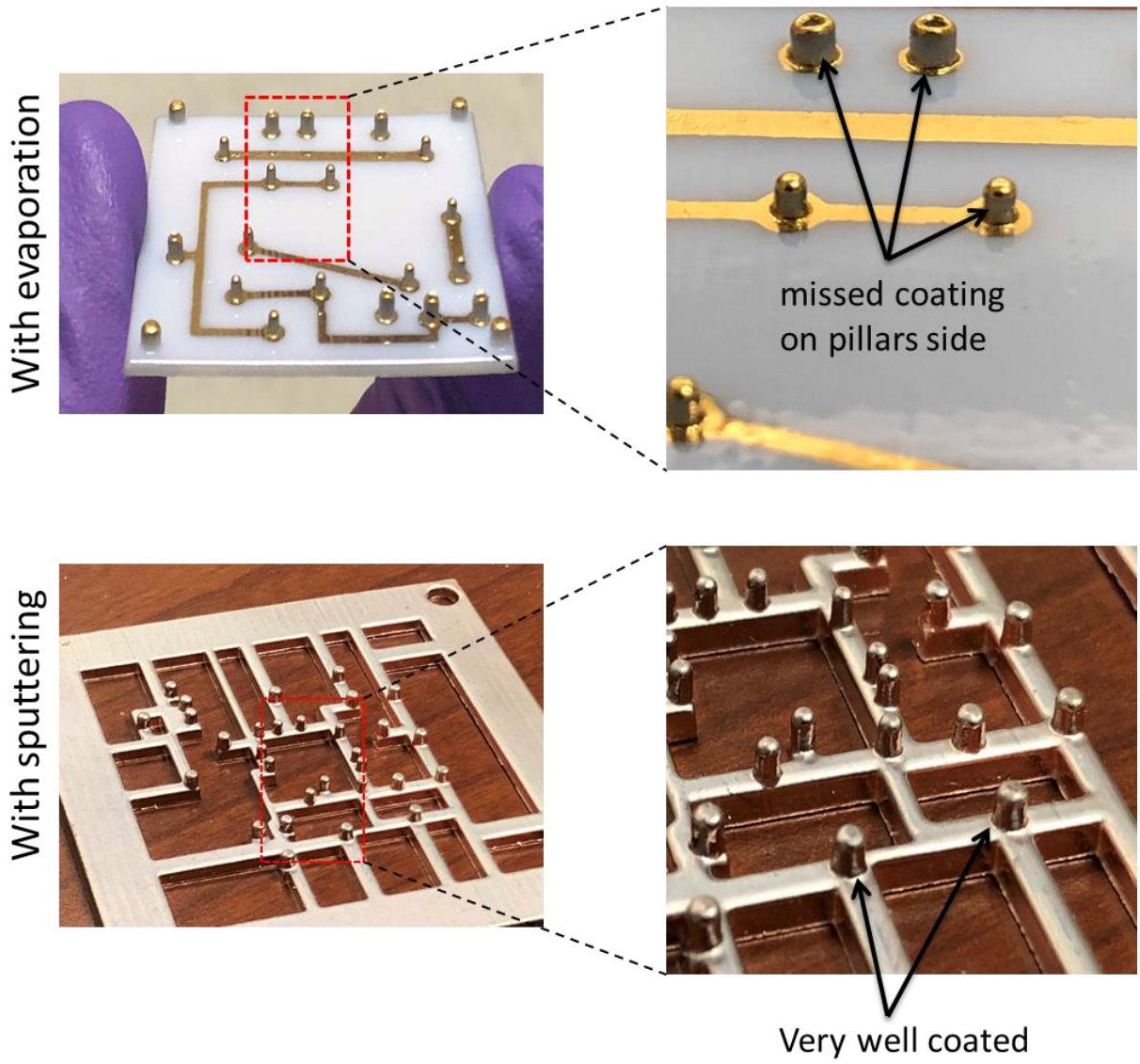

Figure 4. 8: Step coverage with PVD systems for vertical interconnect access

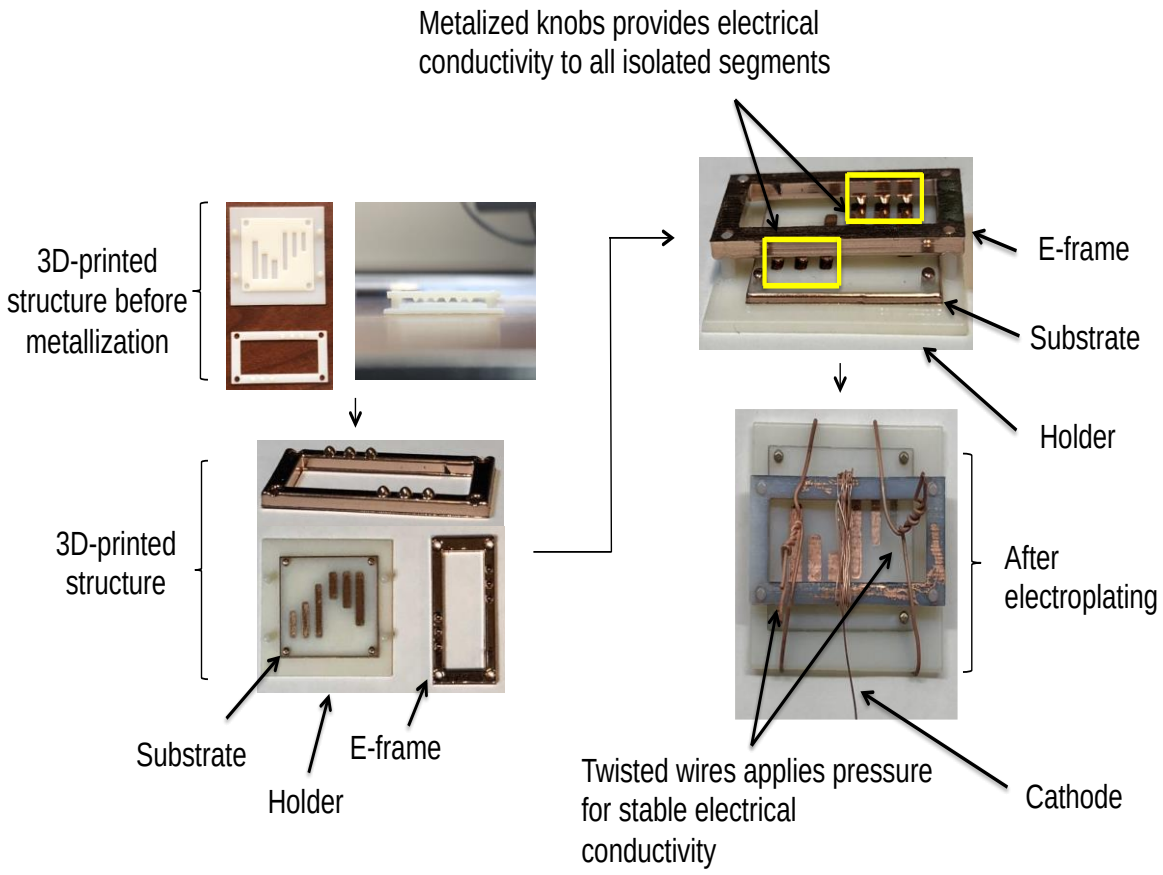

Figure 4. 9: Electroplating process

Chapter 5 3D-printed Microsystem

5.1 Introduction

In this chapter, innovative 3D-printed microsystem is implemented using the process described in chapter 4. First, 3D design of shadow mask, substrate, holder, and electroplating frame is implemented on AutoCAD. The design is based on the schematic of EKG using AD8232 chip and SMD components of the size 0603 (1.6x0.8x0.45) mm. All designs are made with self-alignment feature for fast setup procedure. Second, the designed structures is printed using Object Connex 350 providing good enough resolutions for implementing electronics devices. Third, the demonstrated 3D-printed microsystem for EKG is tested. The ultimate goal of this process is implementing 3D-printed multilayer microsystem, Fig. 5.1.

5.2 Design of 3D-printed Microsystem

In the design of 3D-printed microsystem, several issues were investigated including printer resolutions, vertical interconnect access (via), conductive traces (thin film patterns) and electroplating process. The key part in this technology is a plastic-based self-aligned shadow mask with designated cavity that allows evaporated metal particles to pass through and stick on the substrate layer to create selective metal deposition of broader types of metal target including Cu, Au and Ni.

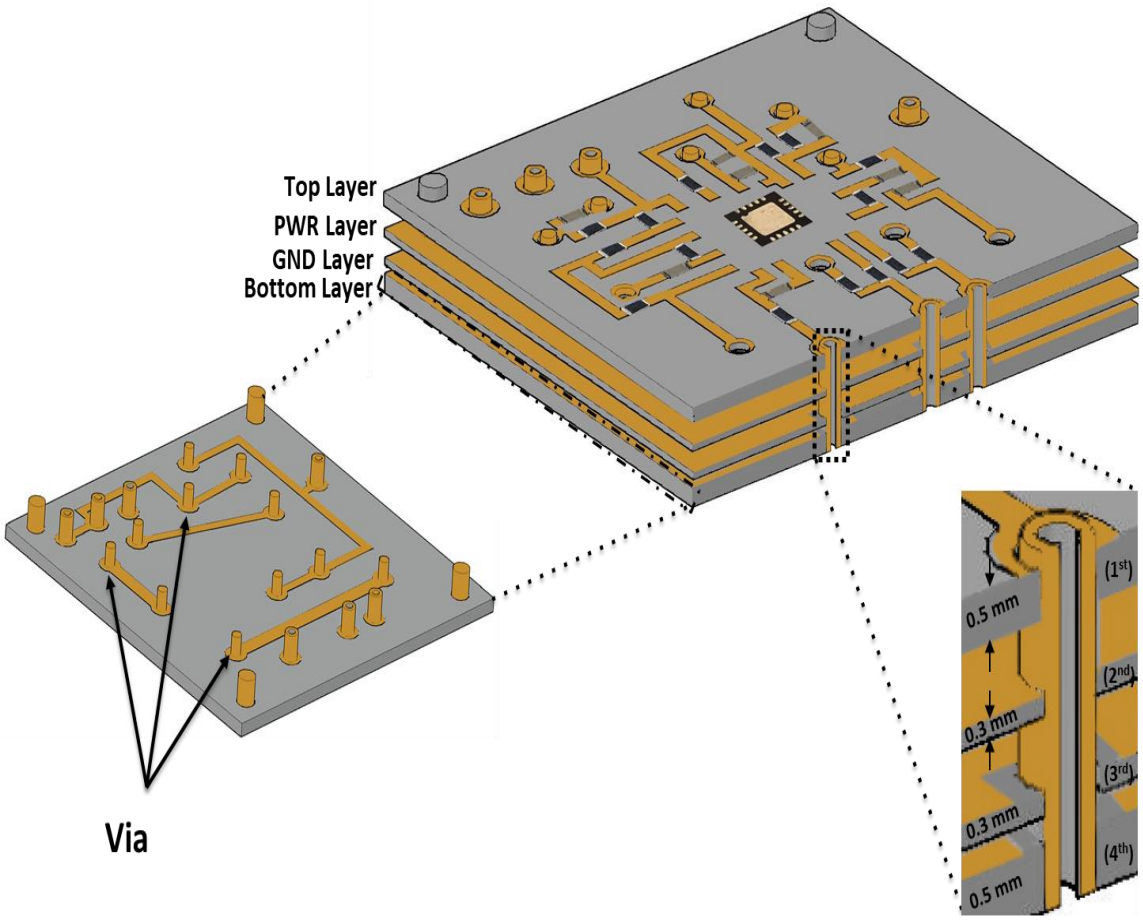

Figure 5. 1: Concept diagram of 3D-printed multilayer microsystem.

This approach provides metal interconnects on plastic substrate more efficiently than conductive inks for the following reasons:

a) By not requiring curing at high temperature to enhance conductivity, it's suitable for wide range of polymer-based substrates.
b) Producing lower resistivity interconnects.

The utilized chip for the initial design (AD8232) mounted bottom-up position for better access the chip pads. Fig. 5.2 shows the concept diagram of the process developed in this work. A) shows a concept diagram of shadow mask (top) with cavity shaping conductive patterns that will be accomplished through Physical Vapor Deposition (PVD) and thin layer printed substrate (bottom) prior to metal deposition. In B), after selectively depositing the interconnects, the substrate placed in the middle of a holder. Then the designed electroplating frame is attached to the holder to create electrical continuity to all deposited films as shown in C). In D, after checking that all conductive traces are connected to cathode lead, then the assembled structure placed in a solution for the electroplating process as discussed in the previous chapter.

Fig. 5.3 shows the concept diagram of components placement and the assembly of two layers of the designed 3D microsystem. Initially, wire bonding was planned to be used for connecting the pads of the chip to the deposited films but since the finished material of the pads was Ten which cannot be bonded then soldering was decided to be performed instead. Au can be deposited on top of the pads then bonding is possible and it is highly desirable for simplicity.

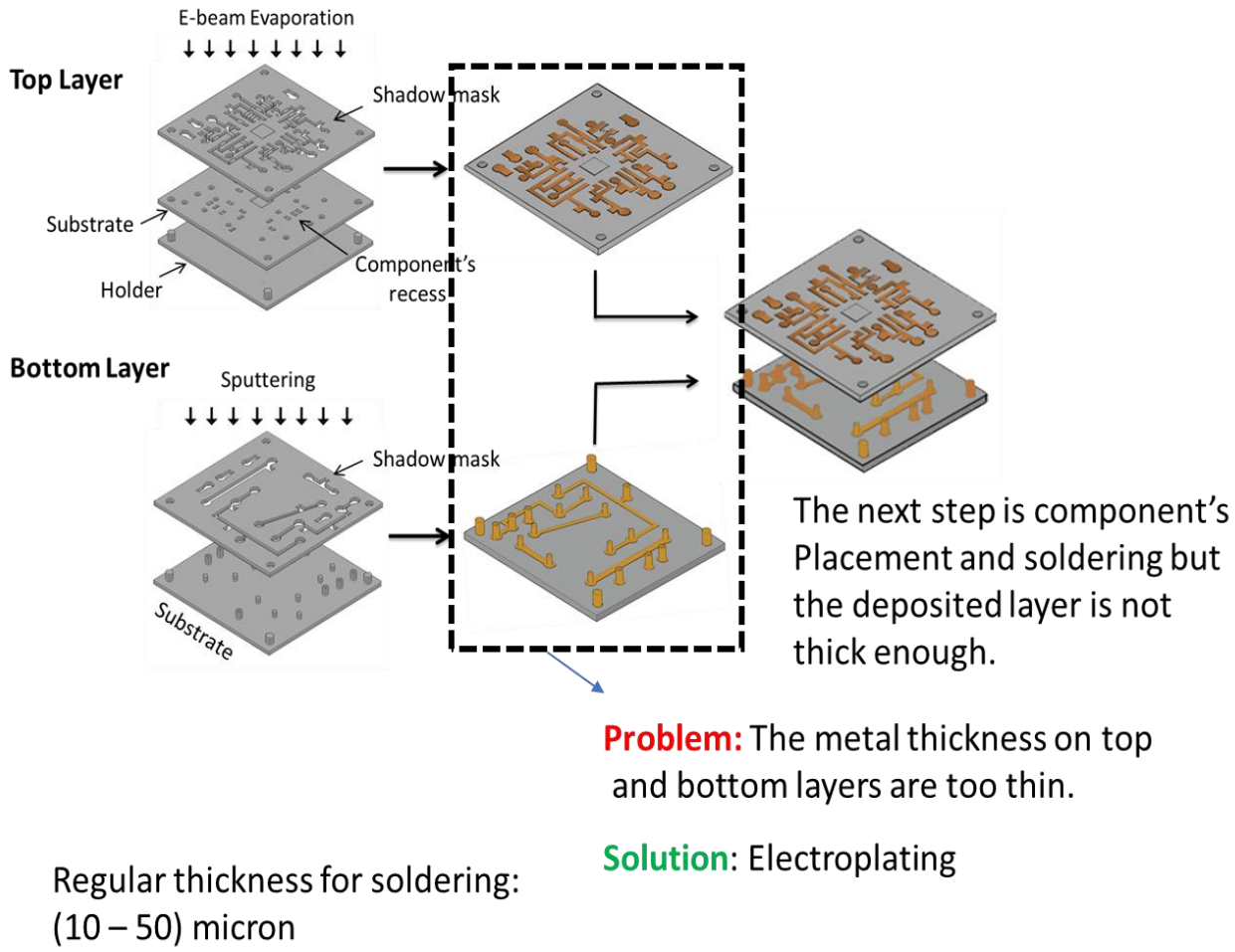

Figure 5. 2: Concept diagram of two layers metallization on 3D-printed substrates

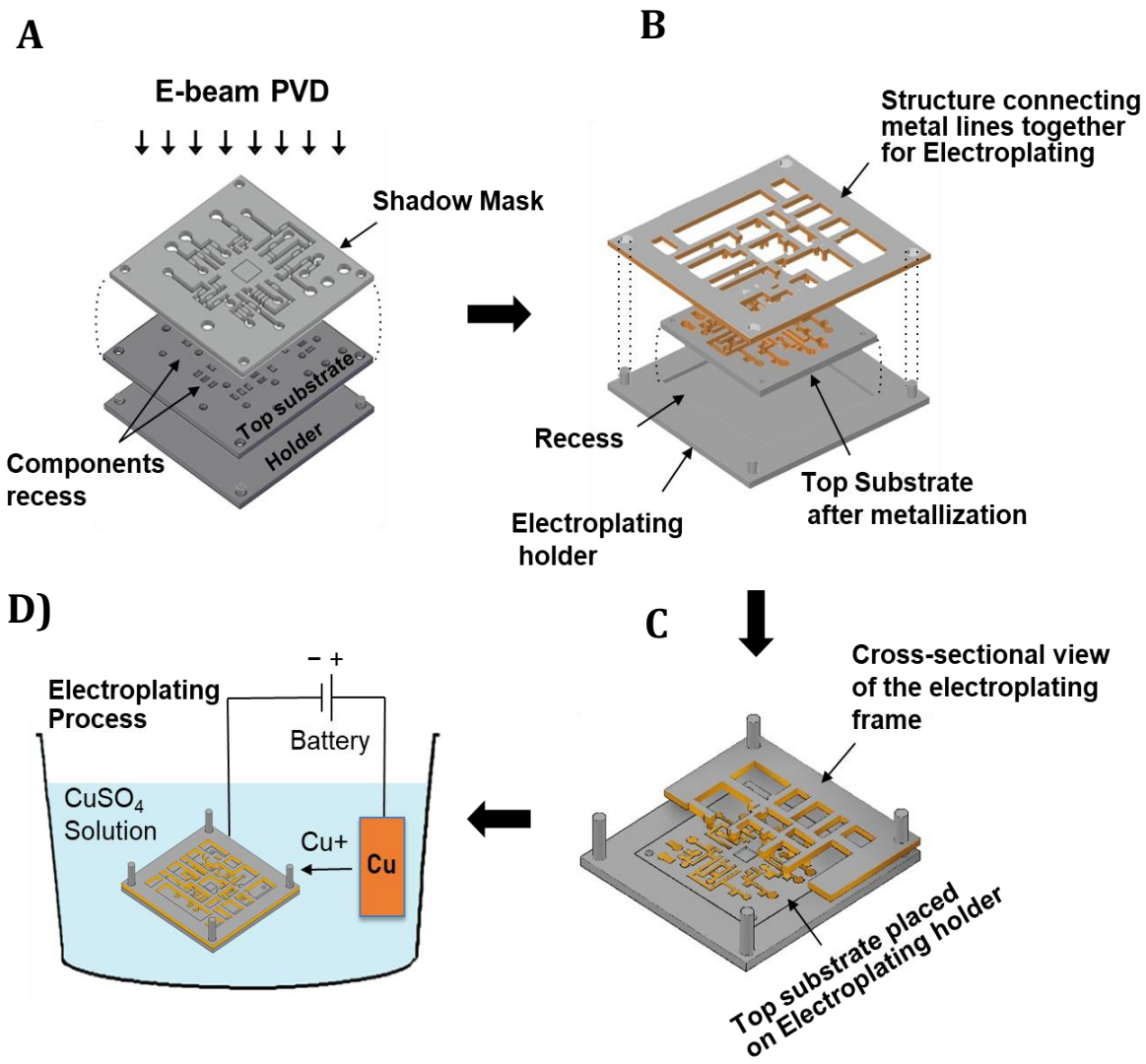

Figure 5. 3: Concept diagram of 3D-printed microsystems processes

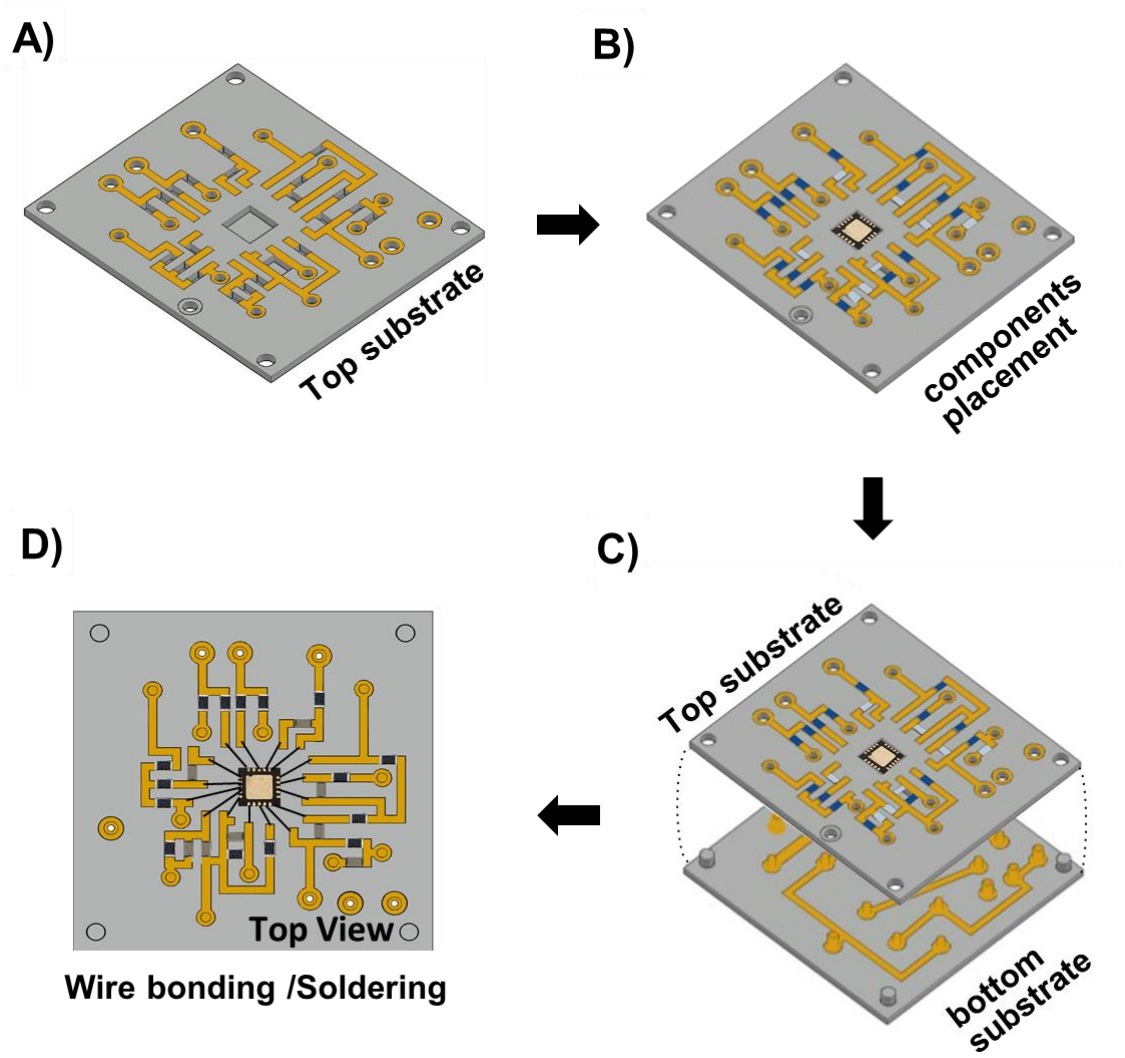

Figure 5. 4: A) Top substrate after electroplating. B) Top substrate after components placement. C) The bottom substrate uses similar process to top substrate which when inserted works as via. D) Top view showing the bonding and/or soldering process.

5.3 Building 3D-printed Microsystem

The main concern for the initial metallization process was on the quality of the adhesion as it represents the key toward implementing good quality deposition on plastic substrate. Therefore, two films were deposited. The first material was Titanium to establish good adessive properties to the printed substrate. The second material was either Gold (Au) or Copper (Cu) to establish high conductive traces. The initial deposition implemented using sputtering which is not directional deposition technique and that results undesired pattern on the substrate. This can be avoided by firmly attaching the designed shadow mask to the substrate and not allowing open space in between.

The desired pattern was first drawn by hand after positioning the chip properly to avoid miss interconnection. There are several trials implemented until the desired patterns achieved.

The first version of microsystem involves two layers of microsystem. As can be seen in Fig. 5.4 A, one shadow mask used for top layer and two shadow masks for second layer. In the first layer, the deposition was successfully implemented, however, the circular trace around the holes (meant for external wire attachment) was not uniformly deposited. This was mainly because of the accuracy of the utilized printer. Therefore, these holes will be increased in diameters for better deposition.

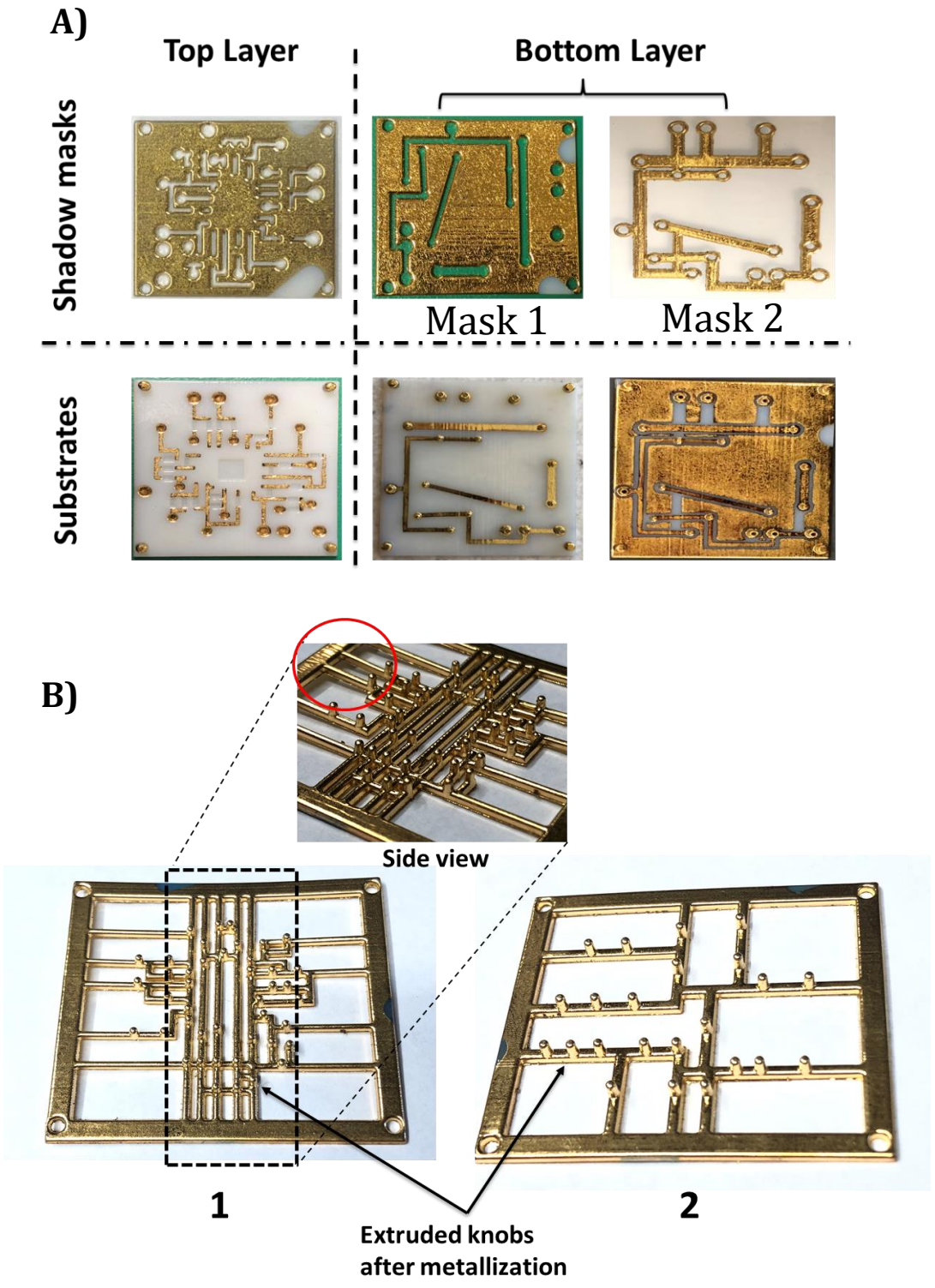

Figure 5. 5: Metal deposition on A) top and bottom substrates, B) electroplating frames for top layer (1) and bottom layer (2).

For the second layer, two shadow masks used, one for thin film deposition and another one for whole layer coating (GND). Since the bottom layer contain vias, it was necessary to apply sputtering with the second mask instead of e-beam evaporation. However, sputtering caused short circuit because some of the deposition passes underneath the shadow mask. Therefore, in the second layer sputtering was implemented with first mask and then e-beam evaporation implemented with the second mask as can be seen in Fig. 5.4 A.

Fig. 5.5 B, shows the metalized electroplating frame for 1) top substrate, and 2) bottom substrate. They are implemented to provide electrical conductivity to cathode lead for electroplating process. The electroplating frame 1, is deformed because two reasons a) almost all the extruded structures are concentrated in the middle area, and b) the thickness of the structure is too thin (1mm). Therefore, the design needed to be improved for 2^{nd} test. The deformation prevents current passing through all isolated metal segments during electroplating.

In the second testing of metal deposition, the traces of the top substrate and bottom substrate were well patterned. However, after the second run deposition some of the metalized vias were scratched on the side when the third mask is displaced. Therefore, another design is needed to hold the shadow mask with dummy pillars instead of functionalized pillars. In addition, these pillars are extruded with 90-degree angle out of the second substrate, this has caused breaking of the deposited film. It's highly recommended to extrude the via with ate least 45-degree angle out of the substrate to avoid this issue Fig. 5.5 A.

The electroplating contact need to be placed on the side of the current path to avoid damaging the deposited film as can be seen in Fig. 5.6 B. During electroplating, it is noticed that the printed material absorbs the electroplating solution which cause the structure to deform and

that may cause miss electrical contact. Therefore, further increase in thickness is needed to delay this deformation until the electroplating time completed.

For third testing, the following are considered:

- The holes of vias on the shadow mask need to be increased in diameter to avoid any interaction during mask removal.
- Ensure conducting of via prior to electroplating, it is highly recommended to change the pillars shape to avoid breaking of the deposited metal.

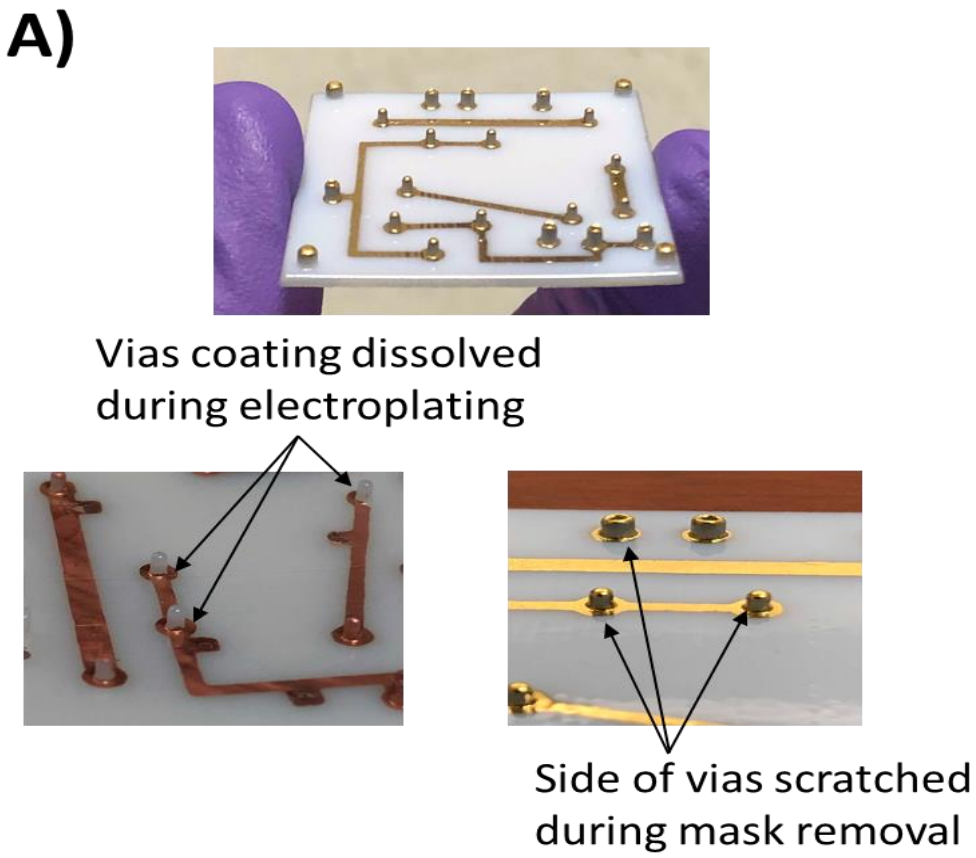

Figure 5. 6: Results of Test 2.

In the third testing of metal deposition, the thickness of the electroplating increased to 2.5 mm to overcome the deformation issue. The pattern was successfully electroplated in some places but others were dissolved in the solution. To solve this issue, uniform pressure is needed to be applied. Therefore, another frame was designed to be placed in top of the electroplating pressure. The resulted electroplating can be seen in Fig. 5.7. Some of the patterns were still dissolving in the solution because of missing electrical contact.

Fig. 5.8, shows the sample preparation of the last trial of electroplating process for 3D-printed microsystem. Because of the issue encountered in trial 3, uniform pressure is applied using two large clips. The electroplating is successfully implemented achieving 8-10 micron thick of copper that is acceptable for soldering process. In this trial several samples were prepared and electroplated. Some of them were electrically conducted to single pad for easier electroplating and then mechanical process used for isolating undesired connection.

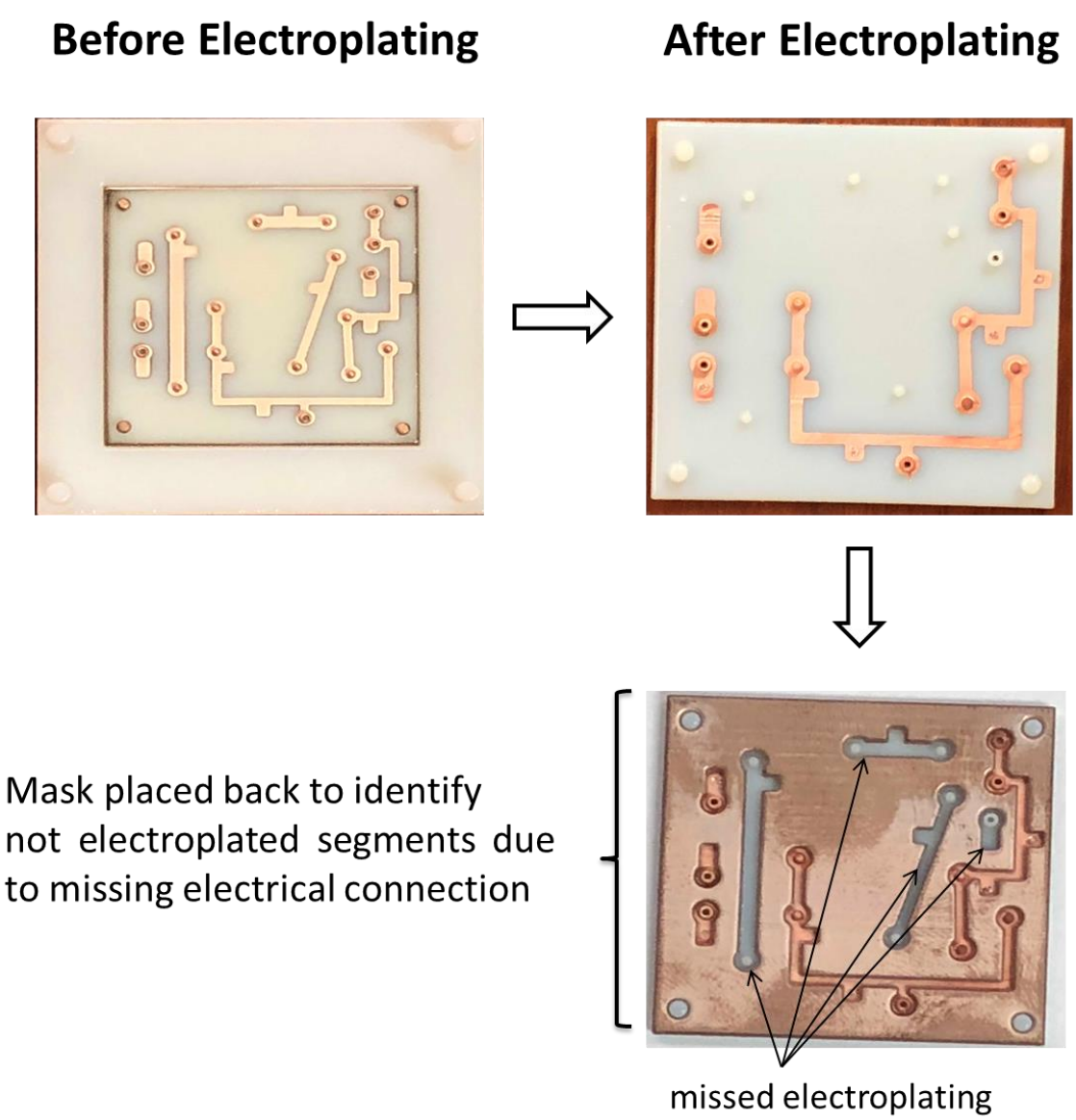

Figure 5. 7: Results of Test 3.

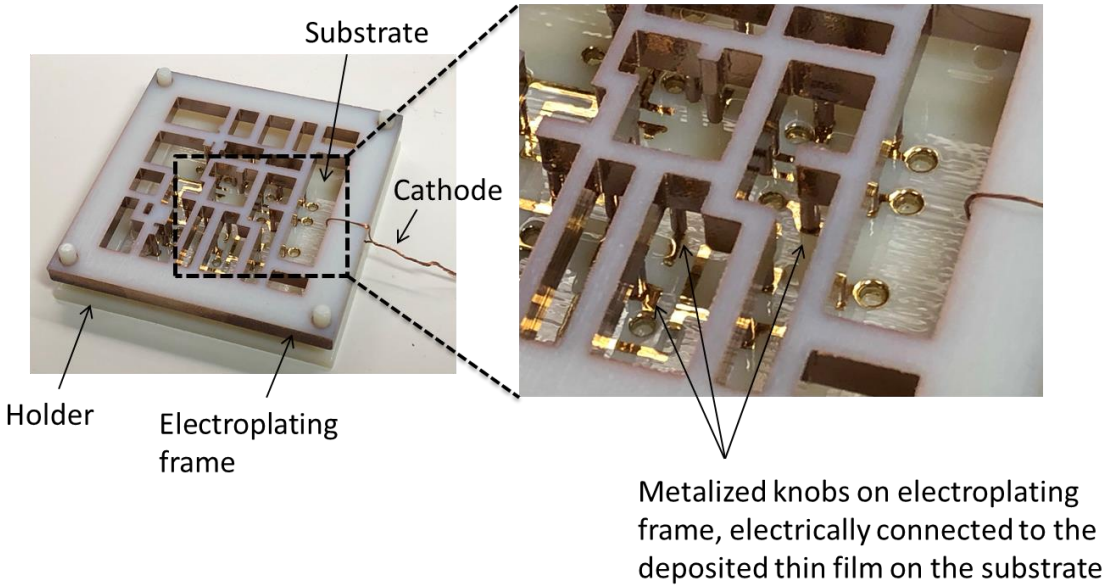

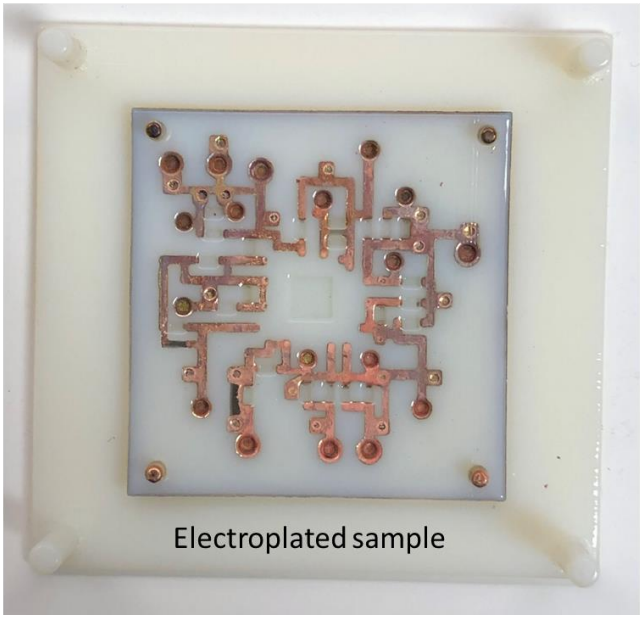

Figure 5. 8: Results of Test 4.

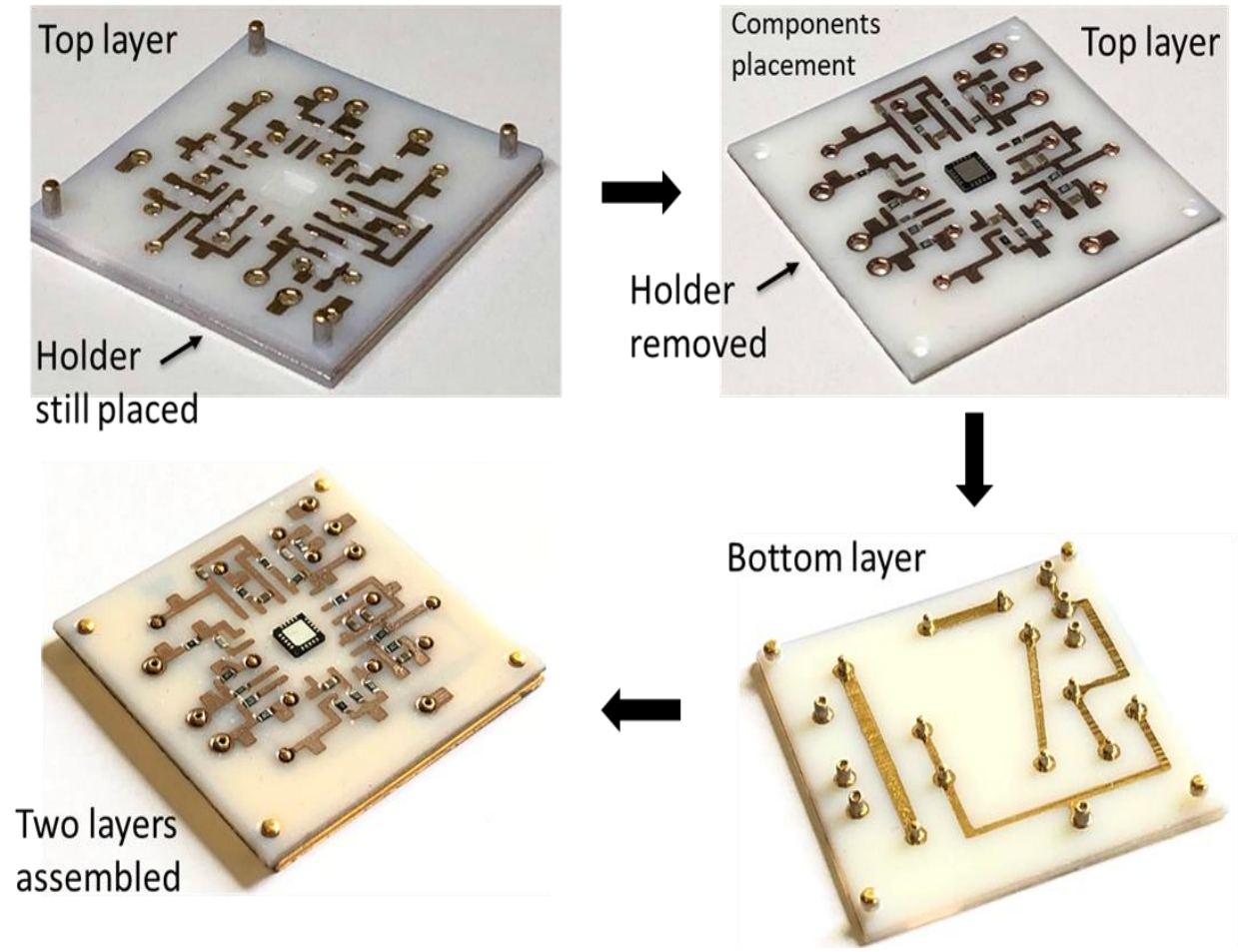

Figure 5. 9: Real images of the developed two layers 3D-printed microsystem.

5.4 Soldering on 3D-printed Microsystem

Soldering is one of the most challenging issue on this work because not only the deposited film thickness is not sufficient, as described in chapter 4, but also the substrate is based on plastic material that cannot handle high temperature. In addition, the utilized chip (AD8232) has very thin pads that are very difficult to solder without a microscope. The width of each pad is 250 nm and the distance between pads is also 250 nm. Therefore, chip soldering implemented very carefully as shown in Fig. 5.8 A). Since the finished material on the chip pad is Ten (Sn) wire bonding cannot be implemented. If the resolution of he printer is high enough to create 250 nm width of aperture, gold (Au) can be deposited on top of the pads to allow wire bonding. Although soldering is the process used in this work, new technique has been slightly demonstrated to overcome soldering issues. The new soldering technique utilizes similar process presented in the previous chapter. In which shadow mask is designed with designated aperture to allow metal deposition. Sputtering is used to interconnect the component with the earlier deposited films on the substrate. As can be seen in Fig. 5.8 B), this process is successfully implemented with 0603 SMD resistor. However, further investigation is required to determine the quality of this new process. It can be implemented simultaneously with the film deposition by proper design of the shadow mask.

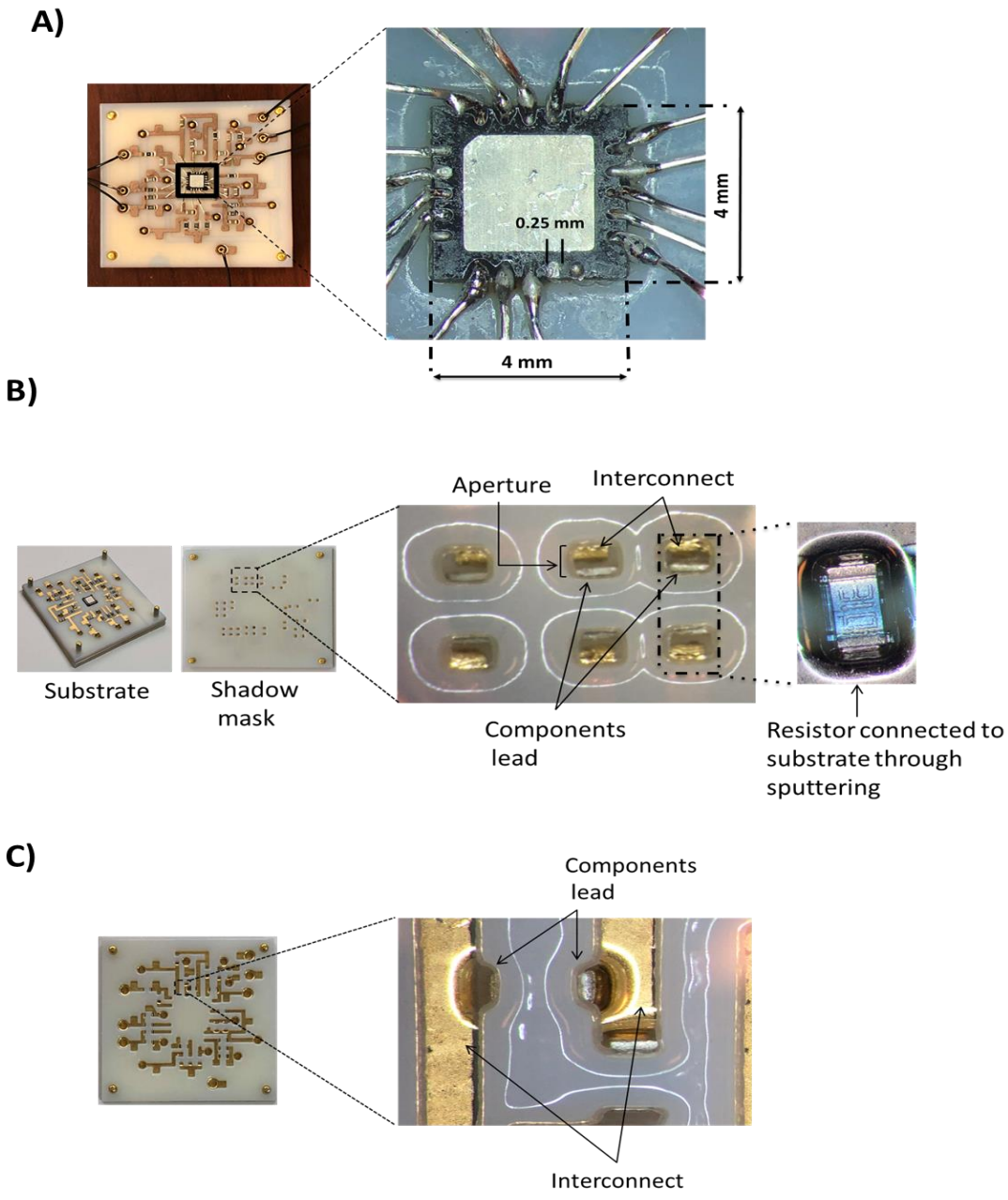

Figure 5. 10: New soldering process for 3D-printed microsystem.

5.5 Testing

To demonstrate the functionality of the proposed process, two microsystems were designed, fabricated and tested. All designs were fabricated based on shadow mask process for thin film patterning. Recess was created on the substrate for components placement. Since the ultimate goal of this work is implementing wearable devices for health monitoring, design of miniature ECG device using AD8232 chip (4mm x4mm) is implemented, see Fig. 5.9.

One of the main advantages of using 3D printing technology is the possibility of printing very high-resolutions geometrics with many different types of materials such as flexible filaments. The developed process in this work can be utilized with many of the 3D-printer filaments. Therefore, a simple test has been implemented to check the flexibility feature using the ne new 3D-printed microsystem process described in this work. One of the concerns in the flexibility of electronics is how far can the device bended without breaking the electrical connection. And what would be the best metal to be utilized for that purpose. In the initial test we have choose copper to be deposited. Fig. 5.11 shows 3D-printed electronics devices implemented with the proposed process. The material used is the polypropylene photopolymer (RGD450). The device thickness is 0.5 mm which is the minimum stable structure thickness can be printed with the Object Connex 350. This small thickness allows the device to be bended to certain range. To identify the flexibility, Light Emitting Diode (LED) is the best option to test the functionality while bending the printed device. Therefore, a new design for 6 parallel LED's is implemented as can be seen in Fig. 5.12. The utilized LED's are SMD 0603 and they were embedded inside the structure by 0.3 mm for better placement. Conductive double side copper tape can be used as sensor element replacing gel-based sensors enabling long term signal aqucsition. Implementing 3D-printed microsystem process in

flexible structure would be successful if the deposited film can be stretchable. Therefore, further studies are needed to investigate the flexible electronics using the process described in previous chapter.

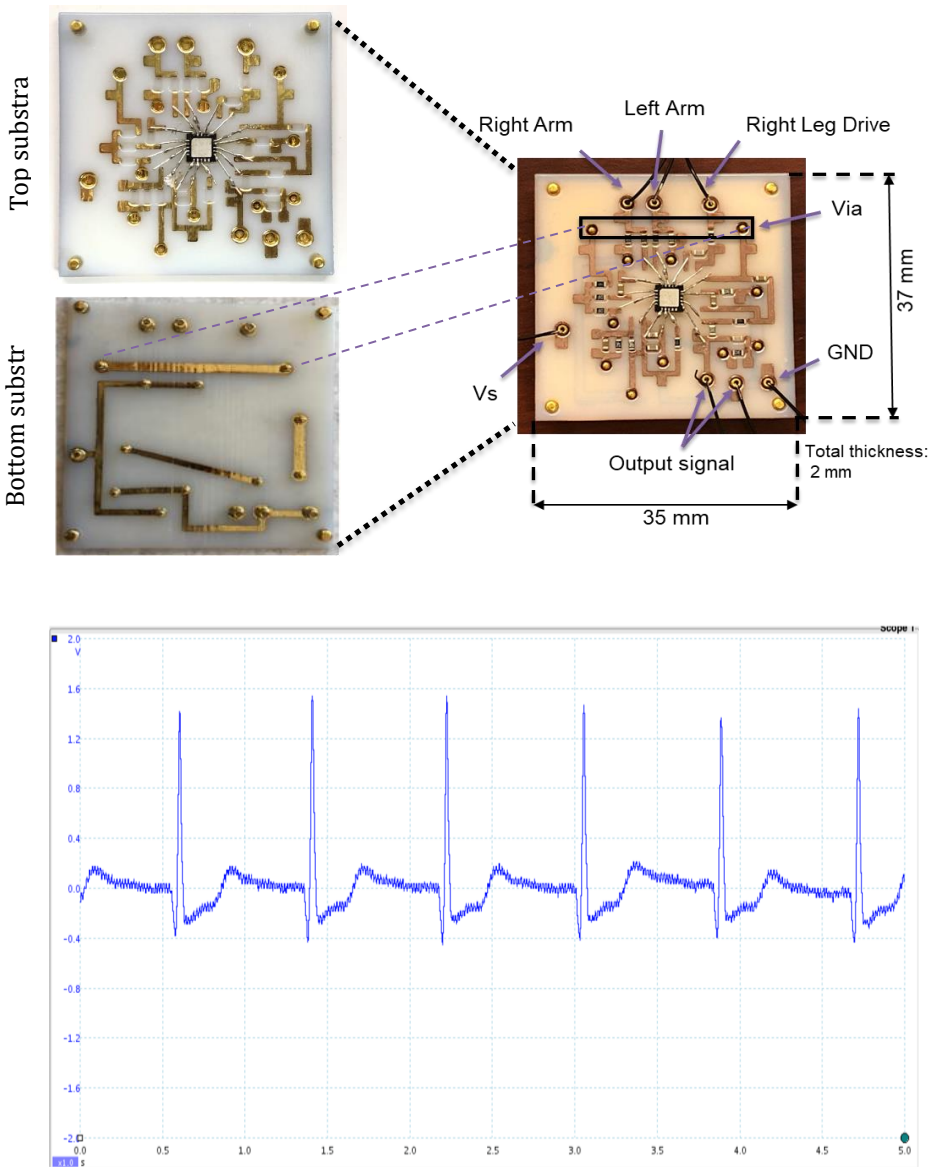

Figure 5. 11: Results of 3D-printed microsystem with Electrocardiogram measurements.

A)

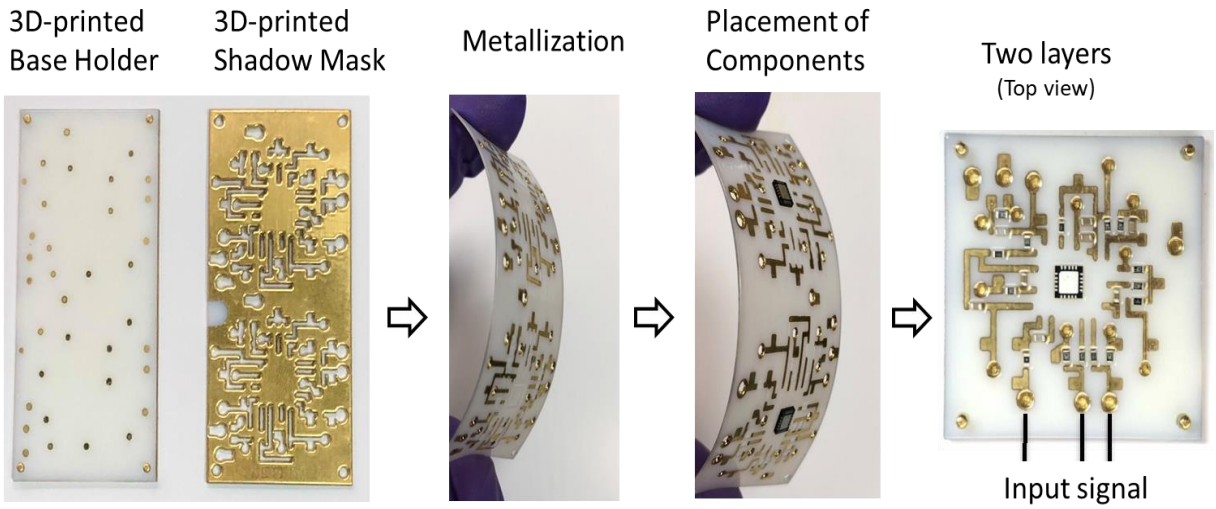

B)

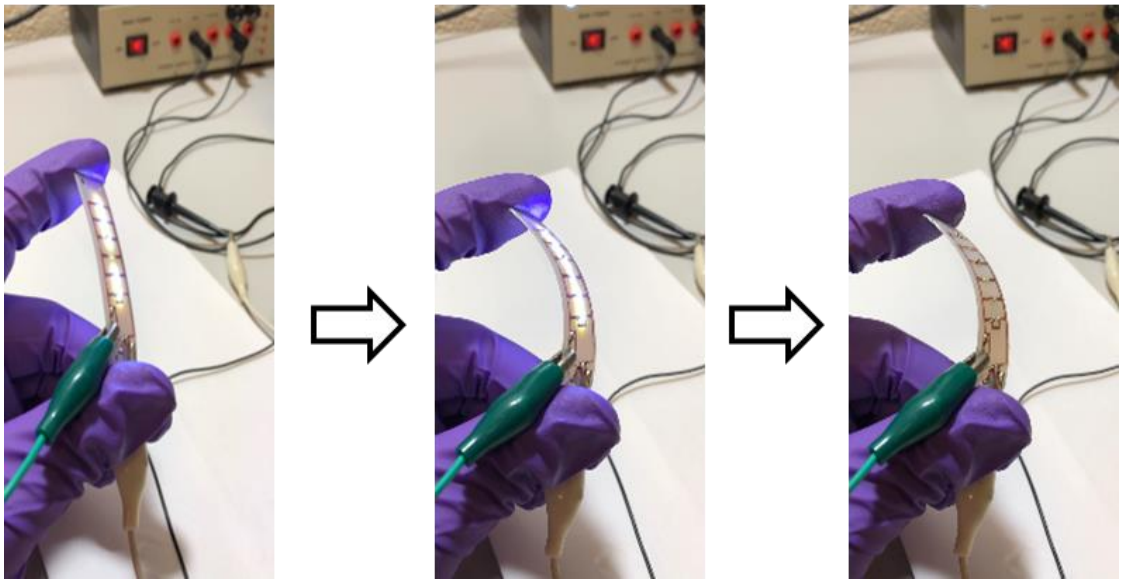

Figure 5. 12: Flexible 3D-printed microsystem.

5.6 Limitations

Since the 3D-printed technology has limited feature sizes, the printed shadow mask was not suitable for cavities lower than 0.35 mm. The utilized chip's pad is 0.25 mm in width, therefore, we considered regular soldering with very tiny wire to join the deposited film with the chip's pad. The other option is to use wire bonding if it is applicable. The AD8232 chip pad is coated with Tin (Sn) which is not suitable for bonding. As the main goal of this work is to implement microsystems on plastic substrate, the shadow mask can be developed with laser cutting machine to achieve very low aperature width. See figure 5.13.

Another limitation of the printed shadow mask is the residue in the aperature area. It requires further cleaning before performing any deposition process. During thin film deposition, the metal particles collides with the resdue preventing uniform pattern on the substrate.

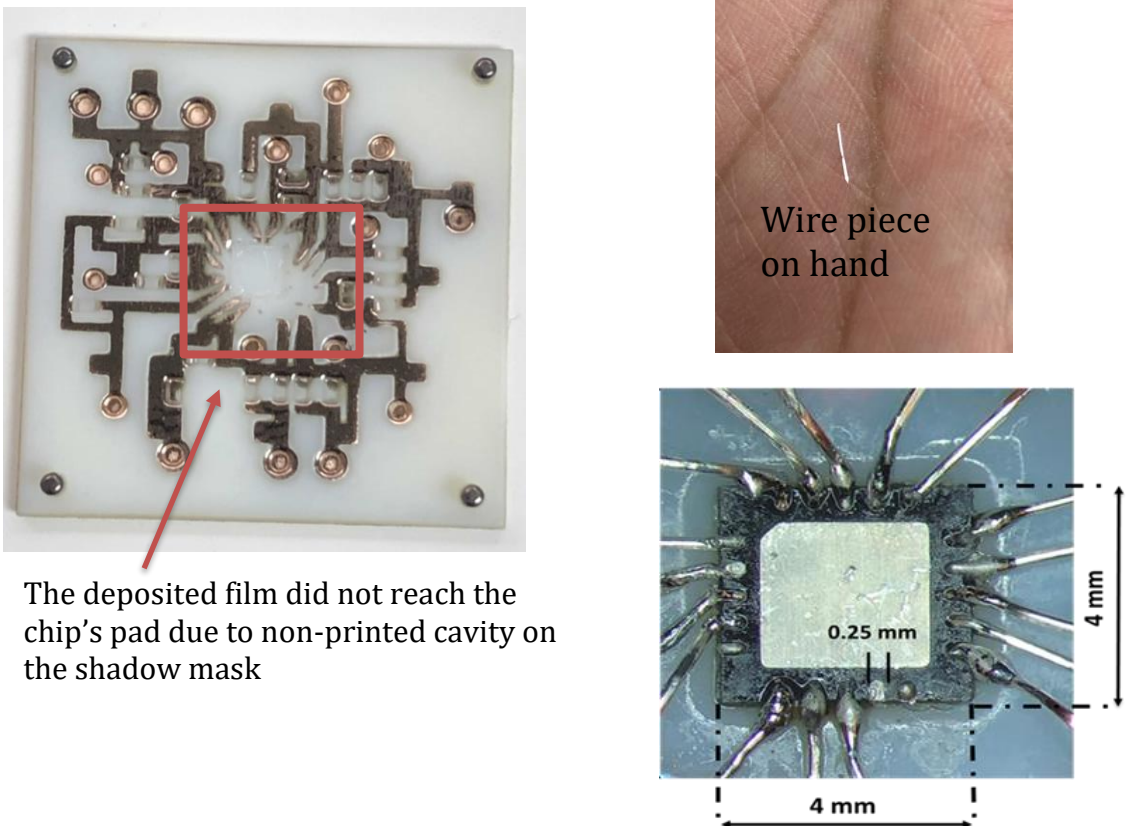

Figure 5. 13: Limitations of the developed 3D-printed microsystem.

Chapter 6 Conclusions and Future Research

6.1 Summary

In this dissertation, we considered design and implementation of a lightweight fabric-embedded EEG/ECG/EMG microsystems for health monitoring and smart home applications. As 3D-printers becoming accessible and wildly spread technology in the world for rapid fabrication of complex geometry objects, they are well suited for mass production of wearable devices. Most of the printed electronics utilizes Cu conductive inks for implementation of electrical connection between electronics components. There is two disadvantages of this process:

1. The conductive ink-based material have high resistivity as compared to bulk material.
2. To lower the resistivity of the conductive ink, it requires curing at high temperature which is not suitable for plastic filaments utilized in 3D-printers.

To solve these issues, evaporated Cu-based interconnects are implemented in this work with unique processes summarized in Fig. 6.1.

To better demonstrate these processes, several tasks are completed as described in chapter 1. In chapter 2, state of the art research work in wearable devices, 3D-printed electronics and bio-sensors are presented. For initial development of 3D-printed multilayer microsystems processes, preliminary results of IEM are produced in chapter 3. Based on these results, ECG microsystem based on single chip (AD8232) was chosen to demonstrate proof of concept of the developed processes. Chapter 4 deals with the details and issues encountered with process development. In chapter 5, Demonstration of the 3D-printed multilayer microsystem for ECG measurements are presented.

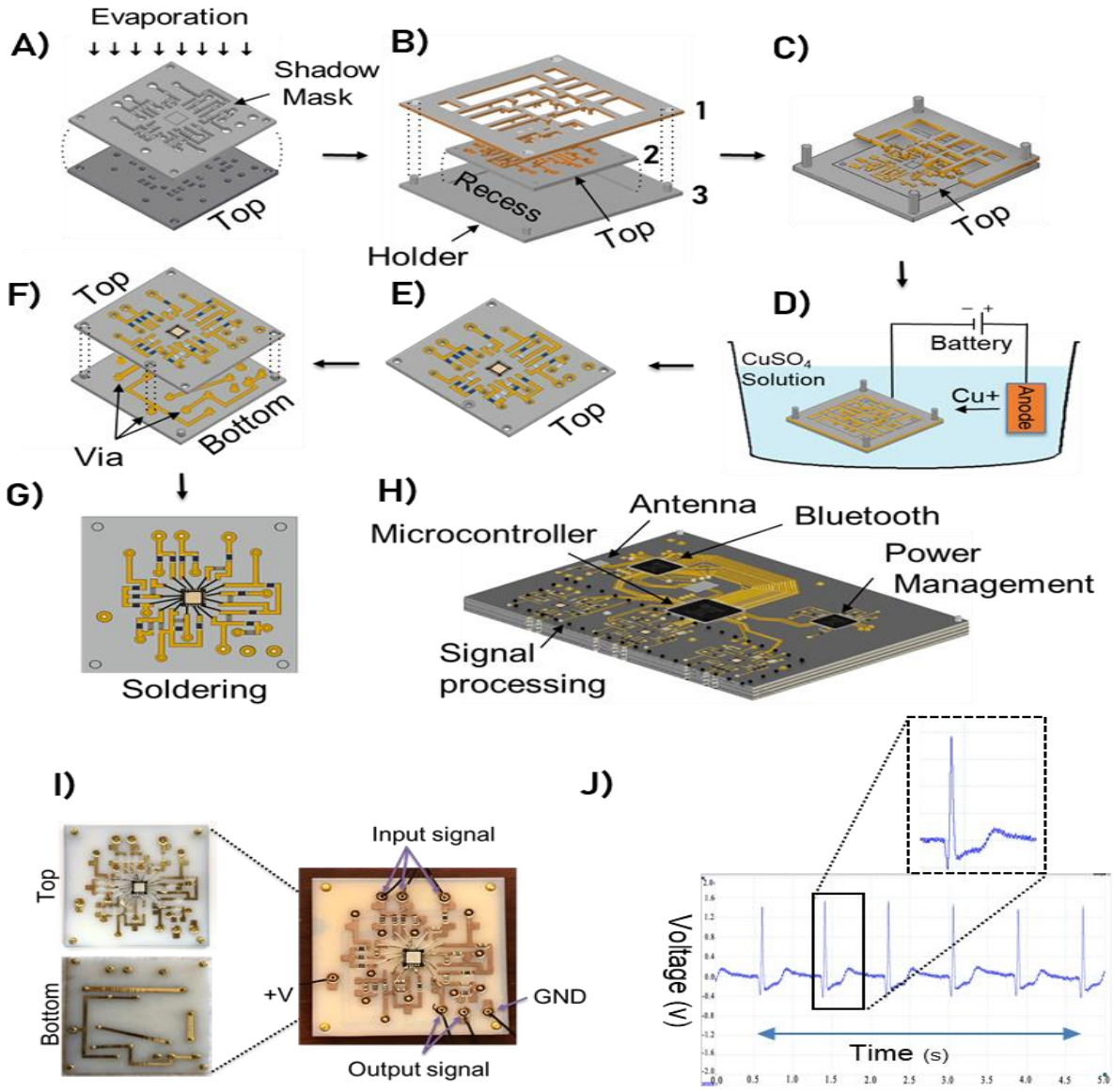

Figure 6. 1: Developed 3D-printed microsystem processes and testing. A) – H) are concept diagrams. A) shadow mask aligned on the top substrate for thin film patterning, B) (1) printed structure with metalized knobs provides temporary electrical connection of the deposited metal films to single lead for electroplating process, (2) top substrate aligned on a holder (3) with recess, C) cross-sectional view showing the temporary electrical connection to the top substrate, D) electroplating process, E) components placement after electroplating, F) the bottom substrate uses process steps similar to top substrate which when inserted provide vertical interconnect access (via) in the implemented two layers microsystem, G) soldering and/or wire bonding, H) multilayer microsystem concept, I) built two layers microsystem with total thickness of 2mm, and J) ECG measured using I).

6.2 Conclusion

In this dissertation, an advancement of high-performance 3D-printed multilayer microsystems processes is presented. The deposited Ti/Au shows a good adhesion to the substrate with good conductive patterns. As the thickness of the deposited films increases with electroplating, the deposited films become more adhesive during soldering if soldering temperature is not too high. A major success of the process requires a high quality adhesive material between the substrate and the deposited metal films. The presented approach provides a low cost and rapid manufacturing for realizing highly integrated and lightweight wearable Microsystems. However, the printing resolutions, the residue in the apertures area, and the surface roughness of the printed filaments are major challenges towards large-scale manufacturing. The minimum aperture width in the shadow mask is 0.3 mm that also represents the width of the patterned interconnects. With proper shadow mask design, this methodology could be applicable for joining electronics components to the substrate during electronics manufacturing process as it provide lower fabrication steps as can be seen in Fig. 6.2.

The proposed approach of 3D-printed Microsystems, reported for the first time, provides highest electrical conductivity in 3D-printed electronics without curing. The integration of physical vapor deposition system with 3D printing machine is very promising for the future industry of 3D-printed Microsystems.

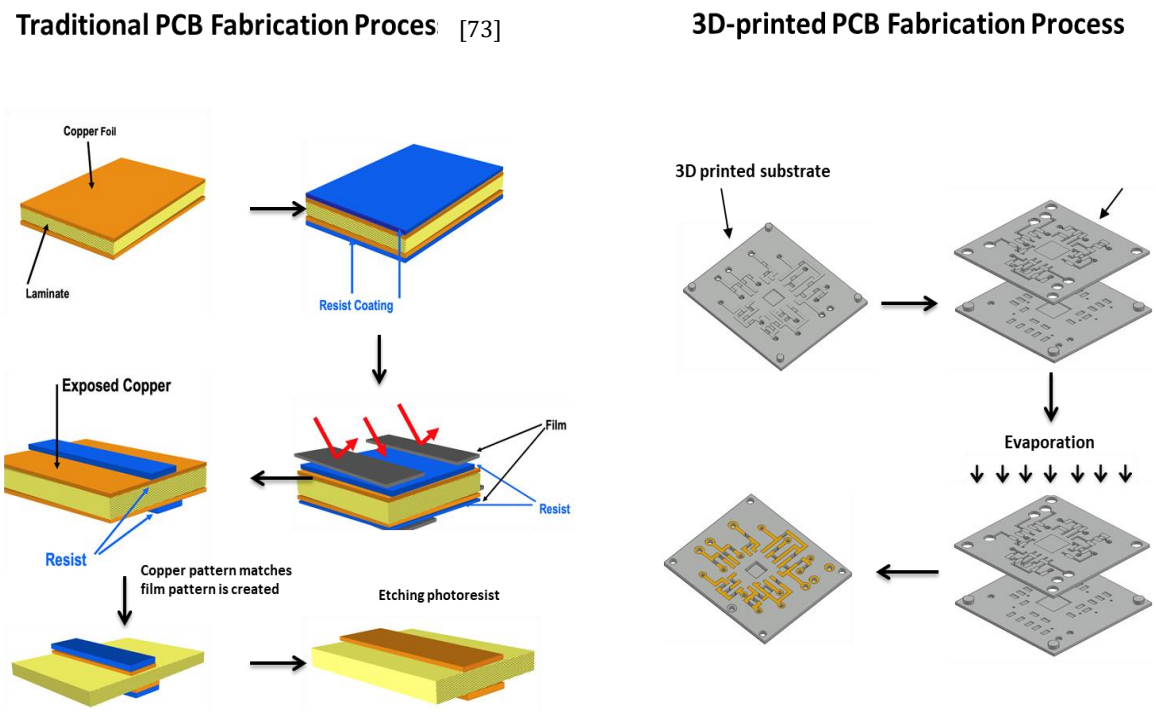

Figure 6. 2: Comparison between traditional PCB fabrication and developed technology.

6.3 Future Research

Since part of the work in this dissertation presents selective metal deposition with 3D printing structures, a combination of 3D printing machine with physical vapor deposition system could be highly considered in the electronics industry. It will provide unique solutions in wide range of applications, especially in manufacturing embedding systems.

In addition, with the recent development of 3D-printed clothes, fabric-embedded sensors can be easily implemented through conductive threads. The ability of printing flexible structures provides opportunity of utilizing the developed process for flexible electronics. It can be utilized in many applications such as smart homes for controlling appliances and health monitoring. Based on the initial testing of flexible electronics in this work, deposition of stretchable and conductive material with high performance is highly desired to avoid film breaking while bonding. Electronics shielding techniques are very necessary for small signal detection and they can easily be implemented with the developed process in this dissertation. Development of space compatible materials in additive manufacturing could also allow utilizing the presented process in aerospace applications. The metallization techniques in this work is not limited to electronics applications. They can be utilized for creating packages with high-shine finishes.

BIBLIOGRAPHY

BIBLIOGRAPHY

[1] Linghu, Changhong, et al. "Transfer printing techniques for flexible and stretchable inorganic electronics." npj Flexible Electronics 2.1:26, (2018).

[2] Schubert, Carl, Mark C. Van Langeveld, and Larry A. Donoso. "Innovations in 3D printing: a 3D overview from optics to organs." British Journal of Ophthalmology 98.2: 159-161, (2014).

[3] Ngo, Tuan D., et al. "Additive manufacturing (3D printing): A review of materials, methods, applications and challenges." Composites Part B: Engineering 143: 172-196, (2018).

[4] Kang, Boseok, Wi Hyoung Lee, and Kilwon Cho. "Recent advances in organic transistor printing processes." ACS applied materials & interfaces 5.7: 2302-2315, (2013).

[5] Li, Yuzhi, et al. "All inkjet-printed metal-oxide thin-film transistor array with good stability and uniformity using surface-energy patterns." ACS applied materials & interfaces 9.9: 8194-8200, (2017).

[6] Gao, Wei, et al. "The status, challenges, and future of additive manufacturing in engineering." Computer-Aided Design 69: 65-89, (2015).

[7] Lewis, Jennifer A., and Bok Y. Ahn. "Device fabrication: Three-dimensional printed electronics." Nature 518.7537: 42, (2015).

[8] Ten Kate, Jelle, Gerwin Smit, and Paul Breedveld. "3D-printed upper limb prostheses: a review." Disability and Rehabilitation: Assistive Technology 12.3: 300-314, (2017).

[9] Tamimi, Faleh, et al. "Osseointegration of dental implants in 3D-printed synthetic onlay grafts customized according to bone metabolic activity in recipient site." Biomaterials 35.21: 5436-5445, (2014).

[10] Mannoor, Manu S., et al. "3D printed bionic ears." Nano letters13.6: 2634-2639, (2013).

[11] Li, Lei, and Y. Yi Allen. "Development of a 3D artificial compound eye." Optics express 18.17: 18125-18137, (2010).

[12] Adams, Jacob J., et al. "Conformal printing of electrically small antennas on three-dimensional surfaces." Advanced Materials23.11: 1335-1340, (2011).

[13] Sun, Ke, et al. "3D printing of interdigitated Li-Ion microbattery architectures." Advanced materials 25.33: 4539-4543, (2013).

[14] Lee, Byoungyoon, et al. "A low-cure-temperature copper nano ink for highly conductive printed electrodes." Current Applied Physics 9.2: e157-e160, (2009).

[15] Salam, Budiman, et al. "Low temperature processing of copper conductive ink for printed electronics applications." 2011 IEEE 13th Electronics Packaging Technology Conference. IEEE, 2011.

[16] Barnat, E. V., et al. "Real time resistivity measurements during sputter deposition of ultrathin copper films." Journal of applied physics 91.3: 1667-1672, (2002).

[17] Lu, Bingheng, Hongbo Lan, and Hongzhong Liu. "Additive manufacturing frontier: 3D printing electronics." Opto-Electronic Advances 1.01: 170004, (2018).

[18] Vatani, Morteza, et al. "Combined 3D printing technologies and material for fabrication of tactile sensors." International Journal of Precision Engineering and Manufacturing 16.7: 1375-1383, (2015).

[19] Chia, Helena N., and Benjamin M. Wu. "Recent advances in 3D printing of biomaterials." Journal of biological engineering9.1: 4, (2015).

[20] Lipson, Hod, and Melba Kurman. Fabricated: The new world of 3D printing. John Wiley & Sons, 2013.

[21] Zardetto, Valerio, et al. "Substrates for flexible electronics: A practical investigation on the electrical, film flexibility, optical, temperature, and solvent resistance properties." Journal of Polymer Science Part B: Polymer Physics 49.9: 638-648, (2011).

[22] Zheng, Xiaoyu, et al. "Multiscale metallic metamaterials." Nature materials 15.10: 1100, (2016).

[23] H.Son,W.S.Park,andH.Kim,"Mobilitymonitoringusingsmarttech- nologies for parkinsons disease in free-living environment," Collegian, 2017.

[24] M. A. Hemairy, M. Serhani, S. Amin, and M. Alahmad, "A comprehen- sive framework for elderly healthcare monitoring in smart environment," Technology for Smart Futures, 2017.

[25] B. SUJATHA and G. AMBICA, "Eeg based brain computer interface for controlling home appliances," International Research Journal of Engineering and Technology (IRJET), vol. 2, pp. 580–585, 2015.

[26] F. Nijboer, E. Sellers, J. Mellinger, M. Jordan, T. Matuz, A. Furdea, S. Halder, U. Mochty, D. Krusienski, T. Vaughan, J. Wolpaw, N. Bir- baumer, and A. Kbler, "A p300-based brain-computer interface for people with amyotrophic lateral sclerosis," 2008.

[27] G. Schalk, D. J. McFarland, T. Hinterberger, N. Birbaumer, and J. R. Wolpaw, "Bci2000: a general-purpose brain-computer interface (bci) system," IEEE Transactions on Biomedical Engineering, vol. 51, no. 6, pp. 1034–1043, June 2004.

[28] A. Nijholt, "The future of brain-computer interfacing (keynote paper)," in 2016 5th International Conference on Informatics, Electronics and Vision (ICIEV), May 2016, pp. 156–161.

[29] N.-H. Liu, C.-Y. Chiang, and H.-C. Chu, "Recognizing the degree of human attention using eeg signals from mobile sensors," in Sensors, 2013.

[30] S. Zhang, J. Gao, and Z. Chen, "Analysis of emotion eeg classification based on ga-fisher classifier," in 2011 First International Workshop on Complexity and Data Mining, Sept 2011, pp. 24–27.

[31] C. Xijun, M. Q. H. Meng, and R. Hongliang, "Design of sensor node platform for wireless biomedical sensor networks," in 2005 IEEE Engineering in Medicine and Biology 27th Annual Conference, Jan 2005, pp. 4662–4665.

[32] Z. Zhi, G. Zhichao, L. Dan, J. Shasha, L. Jiuxing, L. Zhichao, L. Shuichao, J. Tianhai, T. Zhongqun, and Y. C. James, "Translating molecular recognition into a pressure signal to enable rapid, sensitive, and portable biomedical analysis," Angewandte Chemie International Edition, vol. 54, no. 36, pp. 10448–10453, 2015.

[33] W. Kiing-Ing, "A light-weighted, low-cost and wireless ecg monitor design based on tinyos operating system," in 2007 6th International Special Topic Conference on Information Technology Applications in Biomedicine, Nov 2007, pp. 165–168.

[34] M. Sung, C. Marci, and A. Pentland, "Wearable feedback systems for rehabilitation," J. NeuroEng. Rehabil., vol. 2, p. 17, Jun. 2005.

[35] U. Anliker, J. A. Ward, P. Lukowicz, G. Tro¨ster, F. Dolveck, M. Baer, F. Keita, E. B. Schenker, F. Catarsi, L. Coluccini, A. Belardinelli, D. Shklarski, M. Alon, E. Hirt, R. Scmid, and M. Vuskovic, "AMON: A wearable multiparameter medical monitoring and alert system," IEEE Trans. Inf. Technol. Biomed., vol. 8, no. 4, pp. 415–427, Dec. 2004.

[36] B. S. Lin, B. S. Lin, N. K. Chou, F. C. Chong, and S. J. Chen, "RTWPMS: A real-time wireless physiological monitoring system," IEEE Trans. Inf. Technol. Biomed., vol. 10, no. 4, pp. 647–656, Oct. 2006.

[37] C.W.Mundt,K.N.Montgomery,U.E.Udoh,V.N.Barker,G.C.Thonier, A. M. Tellier, R. D. Ricks, R. B. Darling, Y. D. Cagle, N. A. Cabrol, S. J. Ruoss, J. L. Swain, J. W. Hines, and G. T. A. Kovacs, "A multiparam- eter wearable physiological monitoring system for space and terrestrial applications," IEEE Trans. Inf. Technol. Biomed., vol. 9, no. 3, pp. 382–391, Sep. 2005.

[38] J. Ren, C. Chien, and C. C.Tai,“Anew wireless-typephysiologicalsignal measuring system using a PDA and the Bluetooth technology,” in Proc.IEEE Int. Conf. Ind. Technol., Dec. 2006, pp. 3026–3031.

[39] A. Tura, M. Badanai, D. Longo, and L. Quareni, “A medical wearable device with wireless bluetooth-based data transmission,” Meas. Sci. Rev., vol. 3, pp. 1–4, 2003.

[40] J. Mu¨hlsteff, O. Such, R. Schmidt, M. Perkuhn, H. Reiter, J. Lauter, J. Thijs, G. Musch, and M. Harris, “Wearable approach for continuous ECG and activity patient-monitoring,” in Proc. 26th Ann. Int. IEEE EMBS Conf., 2004, pp. 2184–2187.

[41] R. Paradiso, G. Loriga, and N. Taccini, “A wearable health care system based on knitted integral sensors,” IEEE Trans. Inf. Technol. Biomed., vol. 9, no. 3, pp. 337–344, Sep. 2005.

[42] P. S. Pandian, K. Mohanavelu, K. P. Safeer, T. M. Kotresh, D. T. Shakunthala, P. Gopal, and V. C. Padaki, “Smart vest: Wearable multi- parameter remote physiological monitoring system,” Med. Eng. Phys., vol. 30, pp. 466–477, May 2008.

[43] A. Milenkovic, C. Otto, and E. Jovanov, “Wireless sensor networks for personal health monitoring: Issues and an implementation,” Comput. Commun., vol. 29, pp. 2521–2533, 2006.

[44] V. Shnayder, B. R. Chen, K. Lorincz, T. R. F. Fulford-Jones, and M. Welsh, “Sensor networks for medical care,” Division Eng. Appl. Sci., Harvard Univ., Cambridge, MA, Tech. Rep. TR-08-05, 2005.

[45] E. Monton, J. F. Hernandez, J. M. Blasco, T. Herve, J. Micallef, I. Grech, A. Brincat, and V. Traver, “Body area network for wireless patient monitoring,” Telemed. E-Health Commun. Syst., vol. 2, pp. 215–222, 2008.

[46] W. Y. Chung, S. C. Lee, and S. H. Toh, “WSN based mobile u-healthcare system with ECG, blood pressure measurement function,” in Proc. 30th Ann. Int. IEE EMBS Conf., 2008, pp. 1533–1536.

[47] A. Volmer and R. Orglmeister, “Wireless body sensor network for low-power motion-tolerant synchronized vital sign measurement,” in Proc. 30th Ann. Int. IEE EMBS Conf., 2008, pp. 3422–3425.

[48] N. Loew, K.-J. Winzer, G. Becher, D. Scho¨nfuss, Th. Falck, G. Uhlrich, M. Katterle, and F. W. Scheller, “Medical sensors of the BASUMA body sensor network,” in Proc. 4th Int. Workshop Wearable Implantable BSN, vol. 13, pp. 171–176, May 2007.

[49] B. Gyselinckx, J. Penders, and R. Vullers, “Potential and challenges of body area networks for cardiac monitoring,” J. Electrocardiol., vol. 40, pp. S165–S168, Nov. 2007.

[50] Z.Jin,J.Oresko,S.Huang,andA.C.Cheng,“HeartToGo:Apersonalized medicien technology for cardiovascular disease prevention and detection,” in Proc. IEEE/NIH LiSSA, 2009, pp. 80–83.

[51] P. Leijdekkers and V. Gay, “A self-test to detect a heart attack using a mobile phone and wearable sensors,” in Proc. 21st IEEE CBMS Int. Symp., 2008, pp. 93–98.

[52] C.D.Katsis,G.Gianatsas,andD.I.Fotiadis,“Anintegratedtelemedicine platform for the assessment of affective physiological states,” Diagnostic Pathology, vol. 1, p. 16, Aug. 2006.

[53] T. Pawar and S. Chaudhuri, “Body movement activity recognition for ambulatory cardiac monitoring,” IEEE Trans. Biomed. Eng., vol. 54, no. 5, pp. 874–882, May 2007.

[54] C.Peter, E.Ebert,andH.Beikirch,“Awearablemulti-sensorsystemfor mobile acquisition of emotion-related physiological data,” in Proc. 1st Int. Conf. Affect. Comp. Intel. Interaction, 2005, pp. 691–698.

[55] Jane Van Dis. MSJAMA. Where we live: health care in rural vs urban America. JAMA. 2002 Jan 2 , American Medical Association.

[56] K. Morikawa et al., "Compact Wireless EEG system with active electrodes for daily healthcare monitoring," 2013 IEEE International Conference on Consumer Electronics (ICCE), Las Vegas, NV, 2013, pp. 204-205.

[57] M. Poliks et al., "A Wearable Flexible Hybrid Electronics ECG Monitor," 2016 IEEE 66th Electronic Components and Technology Conference (ECTC), Las Vegas, NV, 2016, pp. 1623-1631.

[58] Baek, Ju-Yeoul, et al. "Flexible polymeric dry electrodes for the long-term monitoring of ECG." Sensors and Actuators A: Physical 143.2 (2008): 423-429.

[59] Searle, A., and L. Kirkup. "A direct comparison of wet, dry and insulating bioelectric recording electrodes." Physiological measurement 21.2 (2000): 271.

[60] A. Serteyn, R. Vullings, M. Meftah and J. W. M. Bergmans, "Motion Artifacts in Capacitive ECG Measurements: Reducing the Combined Effect of DC Voltages and Capacitance Changes Using an Injection Signal," in IEEE Transactions on Biomedical Engineering, vol. 62, no. 1, pp. 264-273, Jan. 2015.

[61] Salvo, Pietro, et al. "A 3D printed dry electrode for ECG/EEG recording." Sensors and Actuators A: Physical 174 (2012): 96-102.

[62] Krachunov, Sammy, and Alexander J. Casson. "3D Printed Dry EEG Electrodes." Sensors 16.10 (2016): 1635. ProQuest. Web. 9 July 2018.

[63] B. A. Reyes et al., "Novel Electrodes for Underwater ECG Monitoring," in IEEE Transactions on Biomedical Engineering, vol. 61, no. 6, pp. 1863-1876, June 2014.

[64] Jin, Lang, et al. "Postictal apnea as an important mechanism for SUDEP: A near-SUDEP with continuous EEG-ECG-EMG recording." Journal of Clinical Neuroscience 43 (2017): 130-132.

[65] Wang, Ching-Sung, Chien-Wei Liu, and Yin-Cheng Huang. "ECG monitoring system in vehicles." RF and Wireless Technologies for Biomedical and Healthcare Applications (IMWS-BIO), 2015 IEEE MTT-S 2015 International Microwave Workshop Series on. IEEE, 2015.

[66] T. Le, H. D. Han, T. H. Hoang, V. C. Nguyen and C. K. Nguyen, "A low cost mobile ECG monitoring device using two active dry electrodes," 2016 IEEE Sixth International Conference on Communications and Electronics (ICCE), Ha Long, 2016, pp. 271-276.

[67] A. Alforidi and D.M. Aslam, "Fabric-embedded EEG/ECG/EMG Micro-Systems Monitoring Smart-Home-Occupants' Health/Disease by Smartphones" IEEE International Conference on Electro Information Technology (EIT), May, 2018.

[68] S. T. Kao, H. Lu and C. Su, "A 1.5V 7.5uW programmable gain amplifier for multiple biomedical signal acquisition," 2009 IEEE Biomedical Circuits and Systems Conference, Beijing, 2009, pp. 73-76.

[69] Muth, Joseph T., et al. "Embedded 3D printing of strain sensors within highly stretchable elastomers." Advanced Materials 26.36 (2014): 6307-6312.

[70] Wehner, Michael, et al. "An integrated design and fabrication strategy for entirely soft, autonomous robots." Nature 536.7617 (2016): 451.

[71] Wang, Ziya, et al. "Piezoresistive Sensors: Full 3D Printing of Stretchable Piezoresistive Sensor with Hierarchical Porosity and Multimodulus Architecture (Adv. Funct. Mater. 11/2019)." Advanced Functional Materials 29.11 (2019): 1970067.

[72] Espalin, David, et al. "3D Printing multifunctionality: structures with electronics." The International Journal of Advanced Manufacturing Technology 72.5-8 (2014): 963-978.

[73] Advanced circuits: Printed Circuit Board Manufacturer [4pcb.com].

[74] Campbell, Stephen A. Fabrication engineering at the micro-and nanoscale. 2008.

[75] Du, Tinghao, et al. "Conductive Ink Prepared by Microwave Method: Effect of Silver Content on the Pattern Conductivity." Journal of Electronic Materials 48.1 (2019): 231-237.